Bosque Soil Evaporation Monitoring and Modeling

Final Report

Dr. John Stormont, Principal Investigator
277-6063 **jcstorm@unm.edu**

Dr. Julie Coonrod, Principal Investigator
277-1988 **jcoonrod@unm.edu**

Enrique Farfan, Graduate Student

Kelly Isaacson, Graduate Student

Luke Smith, Graduate Student

Department of Civil Engineering
MSC01 1070
1 University of New Mexico
Albuquerque, NM 87131-0001
Fax: 277-1988

July 11, 2007

1 Introduction

1.1 Background

Evapotranspiration (ET) can be a very significant depletion of water within the Middle Rio Grande corridor. ET includes water consumed by vegetation as well as that evaporated from soil. Attention has been focused on ET depletions from non-native species that have invaded the Middle Rio Grande corridor, notably salt cedar and Russian olive. However, soil water evaporation can be significant, especially in the presence of a shallow water table, and cannot be ignored as an ET component.

Habitat and bosque restoration strategies may include the removal of non-native species. Removal of vegetation can open the ground to more sun and wind, and consequently increase soil water evaporation. Other potential restoration activities include over-banking and creating wetlands, which will increase the near-surface soil moisture content, locally raising the groundwater table and increasing soil water evaporation. Thus, there is a need to understand the magnitude and controls on soil water evaporation as it relates to restoration activities.

Soil water evaporation is maximized if there is a shallow groundwater table, a hot and dry climate, a bare surface exposed to sunlight and wind, and a uniform fine-grained soil. Perhaps the most important factor in the amount of soil water evaporation is the proximity of the water table. If the water table is very shallow (within a meter or so), water will be continually supplied from the water table upward to the soil surface. This type of evaporation is often termed *water table evaporation*. In this case, soil evaporation will be controlled largely by climatic conditions at the soil surface. For example, an increasing amount of shade will greatly reduce the amount of soil evaporation in the presence of a shallow water table.

With a deeper water table, the soil will not be able to transmit water from the groundwater to the surface at a rate sufficient to keep the surface soil wet thus decreasing the evaporation rate. Once the surface soil dries, the amount of water that can be brought to the surface decreases because of the low conductivity of the dry soil, and consequently the evaporation rate drops. In this case, climatic conditions such as the amount of shade may only slightly affect the water table evaporation rate as it is largely controlled by conductivity of the dry surface soil.

In addition to water table evaporation, where the evaporating water is drawn upward from a water table, water that infiltrates at the soil surface can also evaporate. The source of the surface infiltration can be rainfall, snowmelt, surface run-on, or irrigation. In this case, water will be simultaneously drawn into the soil (from gravity and possibly suction gradients) and transmitted from within the soil to the surface to be evaporated. The amount of the infiltrated water that remains in the soil and is not lost to evaporation is a function of many factors, including climate, soil properties, and surface conditions such as mulch or shade. This type of evaporation is referred to herein as *transient evaporation*, as the amount of water in the soil and consequently the

evaporation rate varies with time; one of the more common ways to describe the amount of evaporation from transient evaporation is as a function of the square root time from the last infiltration event. Transient evaporation will occur coincident with water table evaporation.

Despite the significance of soil water evaporation on the water balance, there have been few studies that have quantified soil water evaporation in semi-arid climates. Typically, these studies have focused on evaporation in response to irrigation (Wythers et al., 1999). There are fewer studies of evaporation from a shallow water table (Zammouri, 2001). These studies have largely resulted in site-specific models of evaporation that are not directly applicable to the particular conditions of the Rio Grande Bosque. There has been only one study on soil water evaporation in the Middle Rio Grande, and it was conducted at one location over 30 years ago (ESA, 2003).

1.2 Project summary

A research project involving evaporation monitoring and modeling was undertaken in 2003 by the University of New Mexico and sponsored by the Endangered Species Act Collaborative Program. The overall goal of the project was to develop a method to estimate soil evaporation along the Middle Rio Grande to assess the impact of restoration and rehabilitation decisions on soil water evaporation. The project had three principal components:

1. Collect data for interpretation of soil water evaporative fluxes at various locations along the Middle Rio Grande Bosque.

Soil water content, soil water potential and temperature data were collected at five locations in the Middle Rio Grande bosque. The sites provide conditions of variable soil types, distances to the ground water table, and surface conditions (shade and/or mulch). Data from these locations can be interpreted as evaporative fluxes. We developed a method of interpreting evaporation from limited measurements of water content as suction measurements are very difficult to maintain. We also made complete energy balance measurements at one site for developing and evaluating predictive models of soil water evaporation.

2. Develop an empirical predictive model for soil water evaporation.

A predictive function for water table evaporation was developed from an extensive parametric study of water table evaporation as affected by climate, soil type, and water table distance. The numerical simulation code (UNSAT-L) used for the parametric study simulates transient, multiphase flow including vapor movement. The capability of UNSAT-L to accurately describe evaporation was verified by comparison with field measurements. The resulting function for water table evaporation requires inputs involving soil properties, climate, and distance to the water table.

Four approaches were evaluated for predicting transient evaporation. Data from both a rooftop test and a field test were used to evaluate these methods. The first approach involves simulations using the UNSAT-L program. This approach works well, but requires extensive input and is very computationally intensive. The second approach was a simplified energy balance method that relied on measurements of differential surface temperatures. Predictions of evaporation with this method were considered inadequate, presumably due to some of the assumptions used to derive the methodology. The third approach used a fuzzy logic model developed from the data to predict evaporation. This model was judged to be superior to the differential temperature interpretation method. This method, however, is not amenable to wide scale implementation because it requires substantial training data or calibration in order to be accurate.

The final approach uses a simple water balance model,FAO-56 method, which is widely used for agricultural applications. The capability of the FAO-56 method to estimate bare soil evaporation in the Middle Rio Grande was verified by comparing it to limited field data. Reasonable predictions of evaporation were made with the FAO-56 method using recommended or measured values without extensive calibration.

The FAO-56 method was modified to allow water table evaporation by implementing the predictive equation derived from the parametric study. In this way, we developed a relatively simple and computationally straightforward method for predicting *total soil water evaporation* (transient and water table evaporation). The model also includes the ability to simulate the effect of shade and mulch. This model can be used to evaluate restoration and rehabilitation decisions on soil water evaporation at a particular location.

3. Develop an integrated GIS-based model for estimating soil water evaporation.

The water table evaporation model was made spatially explicit by incorporating the necessary layers in ArcGIS. Water table evaporation is a function of depth to ground water, potential evapotranspiration, and soil properties. As depth to ground water and potential evapotranspiration are also temporally dependent variables, an average monthly model was created. The depth to ground water was determined by calculating a water surface profile for each average monthly flow rate from Cochiti Dam and assuming a horizontal piezometric surface. The monthly potential evaporation grids were created using pan evaporation data. The soil property grids were populated with values from representative bosque soils. This model allows water managers to determine where, geographically, the water budget is most affected by tree removal. Further research resulting in improved data for any of the variables can be easily incorporated into the model at a later date.

1.3 Report organization

Chapter 1 provides a brief background and summary of the project. In Chapter 2, the development of the water table evaporation function is described. A description of

the FAO-56 method is given in this chapter along with a summary of its calibration for Middle Rio Grande bosque location. The modification of the FAO-56 method to include the water table evaporation function is presented, which constitutes the total soil water evaporation model. Chapter 3 describes the application of the total soil water evaporation model at a site adjacent to the Rio Grande near the Albuquerque Diversion Dam. In Chapter 4, the GIS model is presented, and applications using the model are given. Appendix A contains the basis for the water table evaporation function used in both evaporation models. Appendix B contains information about the calibration and validation of the FAO-56 method for estimating evaporation from bosque soils.

1.4 Previous project publications

This report focuses primarily on the second and third project components, namely, the development and application of models for estimating soil water evaporation. Additional information and details regarding the project can be found in the following reports:

Stormont, J., Coonrod, J., Farfan, E., and Harp, D., 2004, "Bosque Soil Evaporation Monitoring and Modeling Report for Year 1," Department of Civil Engineering, report to the ESA Collaborative Program, October 18.

Stormont, J., Coonrod, J., Farfan, E., Harp, D., 2006, "Bosque Soil Evaporation Monitoring and Modeling Report for Year 2," Department of Civil Engineering, report to the ESA Collaborative Program, February 2.

Stormont, J., Coonrod, J., 2005, "Bosque Soil Evaporation Monitoring and Modeling Status Report on Field Monitoring," Department of Civil Engineering, report to the ESA Collaborative Program, May 18

In addition, other publications derived from this project includes:

Harp, D., 2005, Measurement and estimation of soil-water evaporation from bare soil, M.S. Thesis, Department of Civil Engineering, University of New Mexico.

Farfan, E., 2007, Estimating soil water evaporation using nonlinear inverse theory, PhD Dissertation, Department of Civil Engineering, University of New Mexico.

Harp, D., E. Farfan, J.C. Stormont and J.E. Coonrod, 2006. Estimation of Bare Soil Evaporation Using Fuzzy Modeling, ASCE GeoCongress 06, *Session: Sensing methods and devices in geoenvironmental engineering,* February.

Harp, D. R., M.M. Reda Taha, J.C. Stormont, E. Farfan, J. Coonrod, 2006. "Application of Fuzzy Modeling to Estimate Soil-Water Evaporation", *Unsat 06*, ASCE, April, 2268 - 2278.

Farfan, E. J.C. Stormont, D. Harp and J. Coonrod, 2006. Estimating evaporative fluxes in dry climates, *Unsat 06*, ASCE, April, p. 2233 - 2243.

Farfan, E., J.C. Stormont, J. Coonrod,and D. Harp, 2005. "Riparian Restoration Effects on the Middle Rio Grande Water Budget," Proceedings of Watershed Management 2005, ASCE, July.

Harp, D. R., M.M. Reda Taha, J.C. Stormont, E. Farfan, J. Coonrod, 2007. "An evaporation estimation model using optimized fuzzy learning from example algorithm with an application to the riparian zone of the Middle Rio Grande in New Mexico, U.S.A.," *Ecological Modelling*.

2 Evaporation model development

2.1 Approach

The ultimate product from this project is an integrated GIS-based model for estimating soil water evaporation. The GIS model must have the capability to account for spatial and temporal variability of climate, river staging, and soil types to derive maps of the estimated soil water evaporation along the Middle Rio Grande. Consequently, the requirements for the soil water evaporation model included (1) it should be able to account for important properties and conditions related to evaporation, and (2) it should be able to be interfaced with or integrated within a GIS model.

Because soil water evaporation is a complicated physical process involving transient, coupled water-heat flow and phase changes, the requirements and capabilities of a model to reasonably represent the detailed physics of soil evaporation are rigorous. There are numerically based computer models that do include the capability to describe soil water evaporation. Some principal features of these programs include: saturated and unsaturated water movement, including the dependence of soil properties on saturation; water vapor movement; heat transport; and the use of climatic conditions to represent surface boundary condition

The use of these programs requires substantial input, all of which may not be readily available. For example, it is necessary to input information about the soil profile, including layering; hydraulic properties, including unsaturated parameters; and thermal properties, including dependence on water content. With the exception of sites that are the subject of intensive study, knowledge of the layering and properties of the bosque soils are approximate at best. Without knowledge of such detailed input, it is not apparent whether estimates of evaporation would be more accurate with a complex model or a simpler model, and application of a complex evaporation model may not be merited.

These programs are extremely computationally intensive. Solutions are derived from iterative procedures, meaning each time step requires numerous iterations to converge to a solution. Consequently, these programs can require much time; often many hours to find the solution for a simulation for a period of a few days for a single location. This amount of computational time becomes prohibitive for many practical applications.

Another limitation of this type of numerically based computer model is that each application requires discretization of the soil profile that depends on the particular site conditions as well as establishment of convergence criteria and acceptable numerical errors. These numerical considerations affect the error associated with the solution, and require a certain amount of numerical expertise.

The discussion above indicates that while numerical simulations of soil evaporation are valuable, they require too much detailed input and are too computationally intensive to be directly integrated into a GIS model that has a large spatial coverage.

Another approach to predicting evaporation is to use a near-surface water balance model. This type of model does not attempt to describe the details of water movement within soil, but rather generates estimates of evaporation and transpiration from near-surface soil water storage and downward drainage using empirical models. These types of models usually utilize a daily time step. One common approach for modeling water movement, storage and subsquent evapotranspiration in unsaturated soil is based on the concept of "field capacity." Field capacity for a given soil layer is the amount of water that the soil can hold without significant gravity drainage. Once the saturation of the soil layer exceeds the field capacity of the soil layer, excess water moves downward. Field capacity is often described as the water content when gravity drainage from the soil becomes negligible. Estimates of water movement within a soil profile can be made with the field capacity as the principal material parameter for each layer or unit. The field capacity approach implies only gravity-driven (downward) advective water movement. Matric potential gradients, which will affect downward water movement, can result in upward water movement in some cases, and are not accounted for with this approach.

In many water balance models, the soil layering is not explicitly represented, and a single "lumped" root zone is used to describe the near-surface soils. The lumped soil zone has constant soil properties, and vegetation characteristics if transpiration is being considered. Evapotranspiration is usually estimated as a function of the daily climatic demand for water as calculated by the potential evapotranspiration or reference evapotranspiration, the amount of water in the soil, and vegetation characteristics.

Applications of these types of models have shown good agreement with measured data, especially if the model is calibrated to the location (Allen et al., 2005; Mutziger et al., 2005). Advantages of such an approach is that they are computationally much more straightforward than the complex numerical models and require less input. A limitation of this type of approach is that the physical processes are not explicitly included.

When considering predictive model development, it is important to recognize the differences between water table evaporation and transient evaporation. First, water table evaporation can, on some time scale, be reasonably represented as a steady-state process. If the water table depth remains constant, and the climatic demand for water is constant, then upward water movement from the water table to the surface may occur in a steady-state manner, that is, about the same amount every day. A steady-state process suggests that a predictive function independent of time may be developed that reasonably predicts water table evaporation. In contrast, transient evaporation is explicitly a transient process, and must not only account for the effect of the time-dependent quantity of water within the soil on its subsequent movement and evaporation, but also account for the source of infiltration (i.e., precipitation) which itself varies with time.

A second difference between water table and transient evaporation is that one or the other type of evaporation may be of greater interest for intended users of the predictive model. In particular, it is likely restoration decisions will have a greater impact on water table evaporation. Consider two locations under consideration for a restoration activity that would result in bare soil. One location has a much shallower depth to the water table

than the other location. All other factors equal, if this site is cleared, then potentially much more evaporation will occur at the location with the shallower water table.

In addition, the total amount of water lost from water table evaporation could far exceed that of transient evaporation. Transient evaporation will reduce the near-surface soil water content to a low value, and consequently, the evaporation rate will decrease dramatically until another precipitation event. This can often be many days or weeks in the Middle Rio Grande. So, even though the evaporation rate may be great for a short time, the cumulative evaporation may not be great. On the other hand, water table evaporation continues as long the connection between the water table and the atmosphere remains.

Given the considerations discussed above, our approach for predicting soil water evaporation involves developing two different models. These two models are described below.

1. A predictive model for total soil water evaporation using a water balance method that utilizes field capacity and a lumped soil approach.

   This model is able to predict daily water table and transient evaporation at a single location. Daily varying climate, including precipitation, is included. The model is implemented in a spreadsheet, and is not explicitly integrated into the GIS model.

   The steps for developing this method include:

   a. Validating the use of a transient evaporation model (FAO-56 method) for the conditions applicable to the Middle Rio Grande, and
   b. Adding the capability of water table evaporation to the FAO-56 method.

2. A GIS-based predictive model for water table evaporation.

   The GIS model will consequently provide estimates of water table evaporation as a function of water table depth, soil type, and climatic conditions along the Middle Rio Grande. The water table evaporation will vary with time in so much as the water table level and climate changes during the year, but infiltration from precipitation and subsequent transient evaporation is not included.

   The steps for developing this method include:

   a. Validate the use of a computer program (UNSAT-L) to simulate water table evaporation.
   b. Use this computer-program to conduct a parametric study of water table evaporation, varying soil properties, depth to ground water, and atmospheric demand for water.

c. From these results, develop a predictive equation for soil water table evaporation.

If there is sufficient interest from the use of these two models, they could be combined. The magnitude of this effort exceeds the scope of this project.

2.2 Water table evaporation predictive equation

2.2.1 Introduction

A predictive equation was developed from the results of a parametric numerical study of water table evaporation. The numerical simulations were conducted with a program that had previously been used to reproduce water table evaporation experiments under controlled conditions. Additional details are given in Appendix A and in Farfan (2007).

2.2.2 Description of calculations

The computer program UNSAT-L was used to simulate water and vapor movement from a water table through a soil profile, which interacts with the atmosphere. Simulations were conducted with different soil types, water table locations and weather conditions. This program is a modified version of the computer code UNSAT-H (Fayer, 2000). This code was selected because it was readily available and able to be modified to suit the needs of this research. UNSAT-H is an open-source program, which can be modified to satisfy different requirements for output, input and interaction with other programs. UNSAT-L is a product of the modifications performed on UNSAT-H that allows the program to run in different platforms such as UNIX systems. UNSAT-L was able to interface with the program DAKOTA to perform numerous calculations using parallel computing. This was very advantageous, since most of the problems require many hours of simulation.

Because there are infinite possible variations in the field soil profiles, homogeneous soil profiles were used in the majority of the simulations. The soil types selected are those types that could be encountered in the bosque, based on the information provided by the State Soil Geographic (STATSGO) Database from the United States Department of Agriculture, Natural Resources Conservation Service, and soil classification associated with field work for this project. The United States Department of Agriculture (USDA) soil classification system is used in this study. The selected soil types for this study are:

- Loam
- Loamy sand
- Sand
- Sandy loam
- Silt loam

The van Genuchten soil hydraulic model was used to describe the hydraulic

properties of the different soils. Because of its widespread use in the solution of problems involving water movement in soils, information about soil type and corresponding van Genuchten parameters can be found in the literature for many soils. A soil hydraulic parameter database was generated from published literature, and used to assign soil hydraulic parameters for each simulation.

The simulations included the effects of heat flow, and thus are referred to as thermal solutions. The thermal solution requires input of daily air temperature, vapor density and wind speed. Fick's equation accounts for the effects of the three factors on the soil water evaporation rate. An increase in the soil temperature results in an increase in the vapor density at the soil surface and an increase in the vapor density gradient between the soil and the atmosphere resulting in an increase of the evaporation rate. A dry soil surface has a lower vapor density as a consequence of a reduction in the vapor density gradient between the soil surface and the atmosphere, producing a reduction in the evaporation rate. The atmospheric vapor density and the atmospheric boundary-layer resistance controls the process of transporting water vapor from the soil surface to the atmosphere. This atmospheric boundary layer is defined as the region near the soil surface that it is directly affected by the soil surface conditions. For example, if the wind velocity decreases, the evaporation rate is reduced.

The soil thermal properties are defined from general soil mineral properties and the vapor properties, which are referred to as the thermal properties of water vapor. Fourier's law is used to model heat conduction in the soil and Fick's law is used to simulate vapor diffusion.

The soil is modeled in one direction (vertical). The computer code uses modified Picard iteration, a finite difference approximation, to solve the constitutive equation. A discretization of the soil profile is defined, where the node spacing is very small near the surface and becomes progressively larger downward through the soil profile.

Two boundary conditions are specified for each analyzed soil profile. The upper boundary condition represents the soil-surface-atmosphere interaction. The required input in the numerical model is daily weather data for a thermal solution. The lower boundary condition represents the location of the water table. This condition is represented by setting the lower node to a constant head equal to zero; this condition corresponds to a static water table. For each soil type and climate set, the water table depth was varied between 200 mm to 2.5 m. A saturated soil profile and a temperature equal to 275 K were used as initial conditions for each simulation.

For each soil type and each water table depth, three daily PET values were used in the simulations to represent a range of daily climate conditions that may be expected in the middle Rio Grande valley. From examination of weather data from weather stations in the Middle Rio Grande Valley, PET values of 10, 6 and 4 mm/day were selected to describe reasonably typical PET values observed in the bosque for summer, spring-fall and winter. These values were selected to encompass high, medium and low values of PET.

The simulation time used was 365 days. This simulation time ensures that a pseudo steady state is achieved, where the upward flow from the water table is equal in magnitude to the evaporation rate.

2.2.3 Results

Examples of results are given in Figures 2.1 through 2.4. Complete results along with corresponding soil properties are given in Appendix A. The results reveal that the evaporation rates can change dramatically as a function of soil type and properties as well as distance to the water table. For many soils, at very shallow distances to the water table, the evaporation rate levels off at a limiting value. This evaporation is limited not by the soil, but by the atmospheric demand for water (i.e., PET). The evaporation rate decreases when the ability of the soil to transmit water upward from the water table to surface decreases below the atmospheric demand for water. Some soils are able to transmit water from a water table as deep as 1 m before the evaporation rate decreases; whereas the evaporation rate from other soils decreases to low values even when the water table is shallow.

The numerical simulation results were compared to Gardner's solution. Gardner's solution is a well-known closed-form solution for water table evaporation (Gardner, 1958; Jury et al., 1991). Figure 2.5 shows a comparison of soil water table evaporation rates for a loam soil with a PET equal to 10 mm/day. Gardner's equation overestimates the evaporation rate by orders of magnitude compared to the results obtained with UNSAT-L. For example Gardner's equation predicts an approximate evaporation rate equal to 10 mm/day for a water table equal to 1 m from the soil surface, while UNSAT-L with an equivalent PET = 10 mm/day predicts an evaporation rate equal to 0.6 mm/day for the same water table location.

The discrepancy between UNSAT-L and Gardner's equation is due to differences between these two approaches. Gardner's equation predicts the maximum possible evaporation rate above a water table due to movement of water in the liquid phase. Since Gardner's equation only considers water movement in the liquid phase and neglects the water movement in the vapor phase, this equation is only applicable when the water content is relatively great near the surface. UNSAT-L considers the contribution of the vapor flow to the evaporation rate. In contrast to Gardner's solution, the UNSAT-L solution includes thermal effects. Another important consideration is that Gardner's equation is independent of climatic conditions; UNSAT-L accounts for temperature and solar radiation variations during a day. UNSAT-L restricts the maximum evaporation rate to the PET, whereas there is no limitation on the evaporation rate with Gardner's equation.

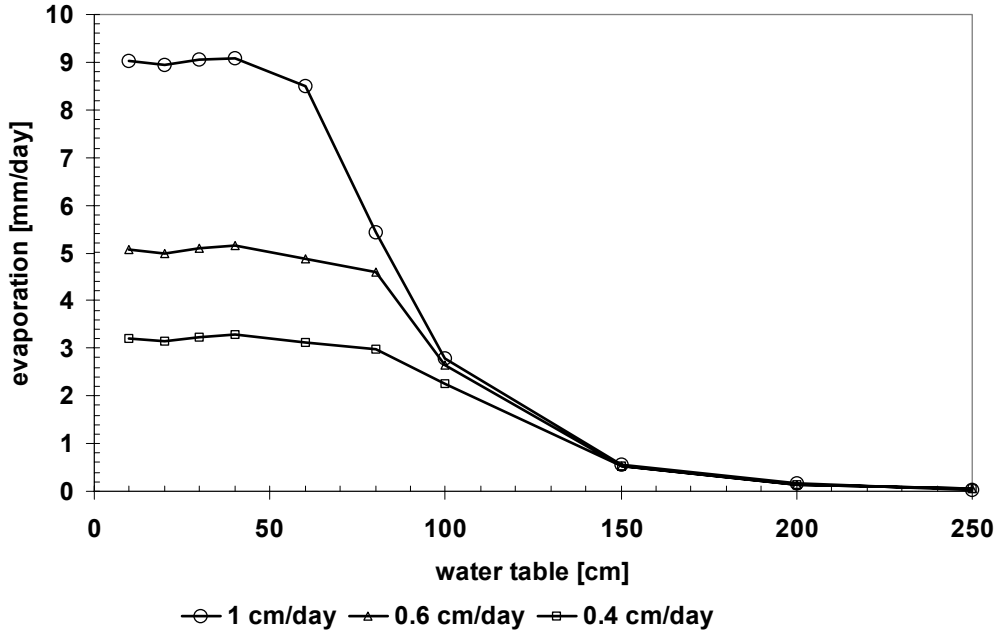

Figure 2.1 – Evaporation rate as a function of water table depth for three values of daily PET. Soil type was loam sand c . Details of calculations and soil properties are given in Appendix A.

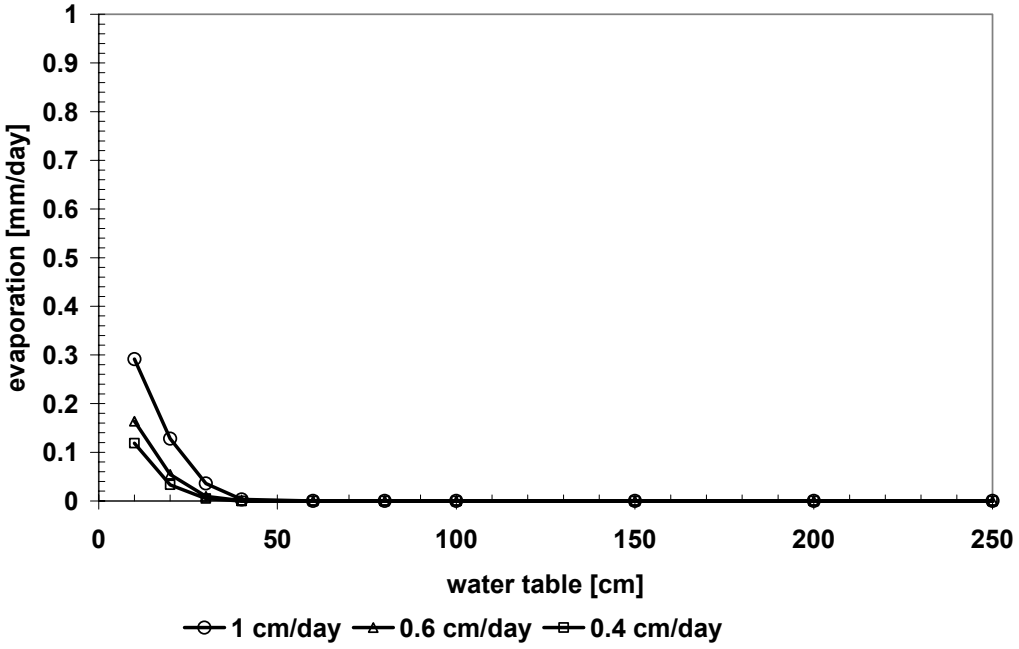

Figure 2.2 – Evaporation rate as a function of water table depth for three values of daily PET. Soil type was sand c . Details of calculations and soil properties are given in Appendix A.

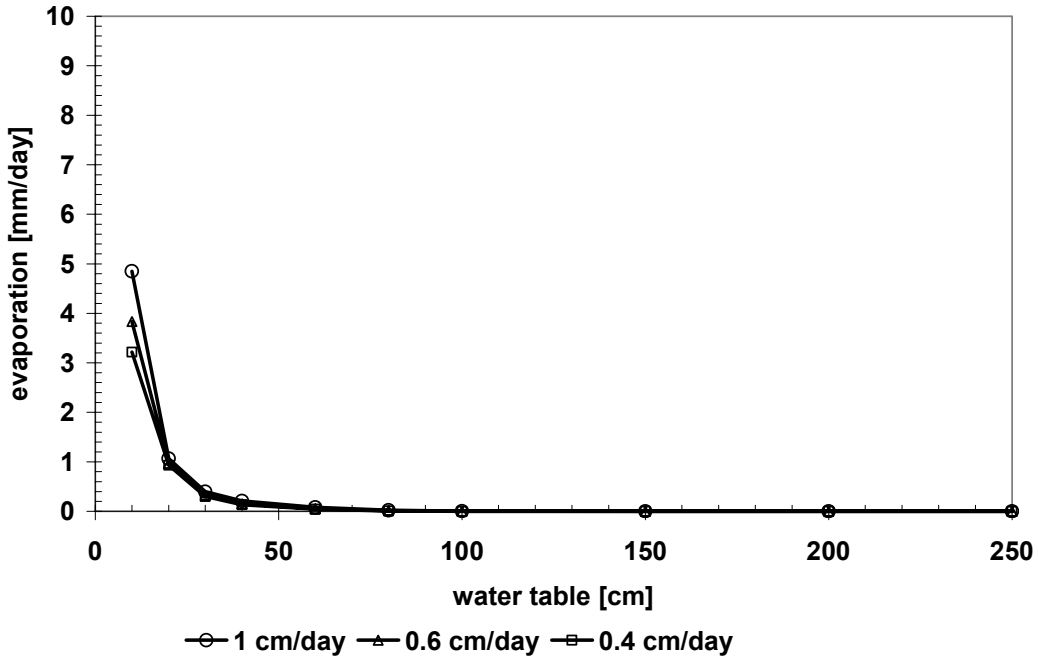

Figure 2.3 – Evaporation rate as a function of water table depth for three values of daily PET. Soil type was sand d . Details of calculations and soil properties are given in Appendix A.

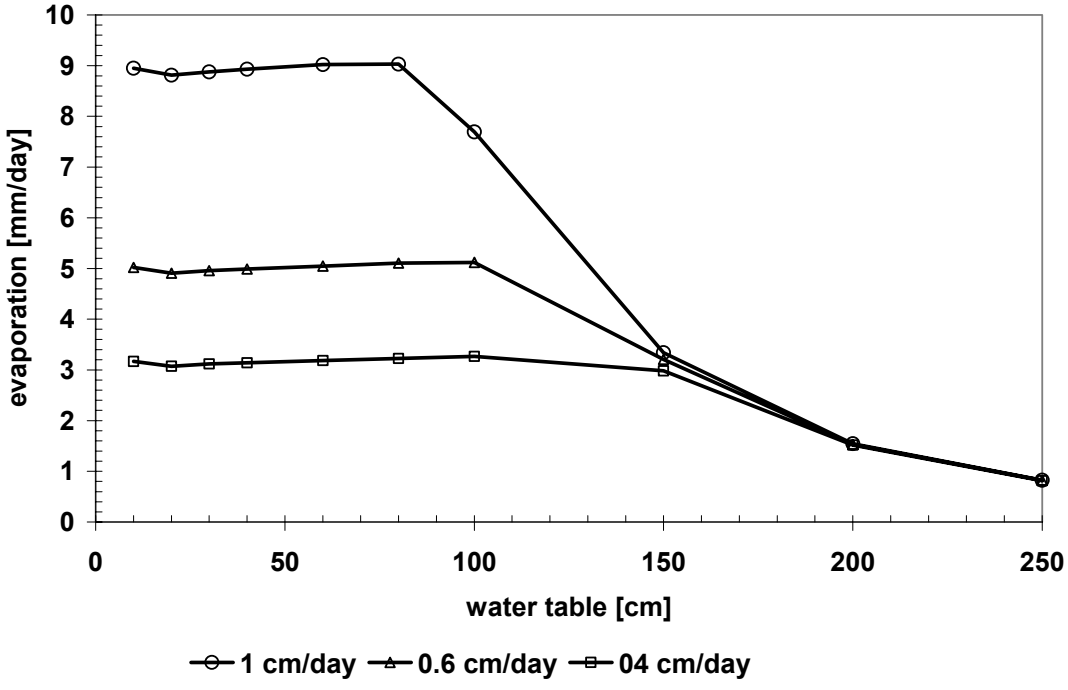

Figure 2.4 – Evaporation rate as a function of water table depth for three values of daily PET. Soil type was sandy loam d. Details of calculations and soil properties are given in Appendix A.

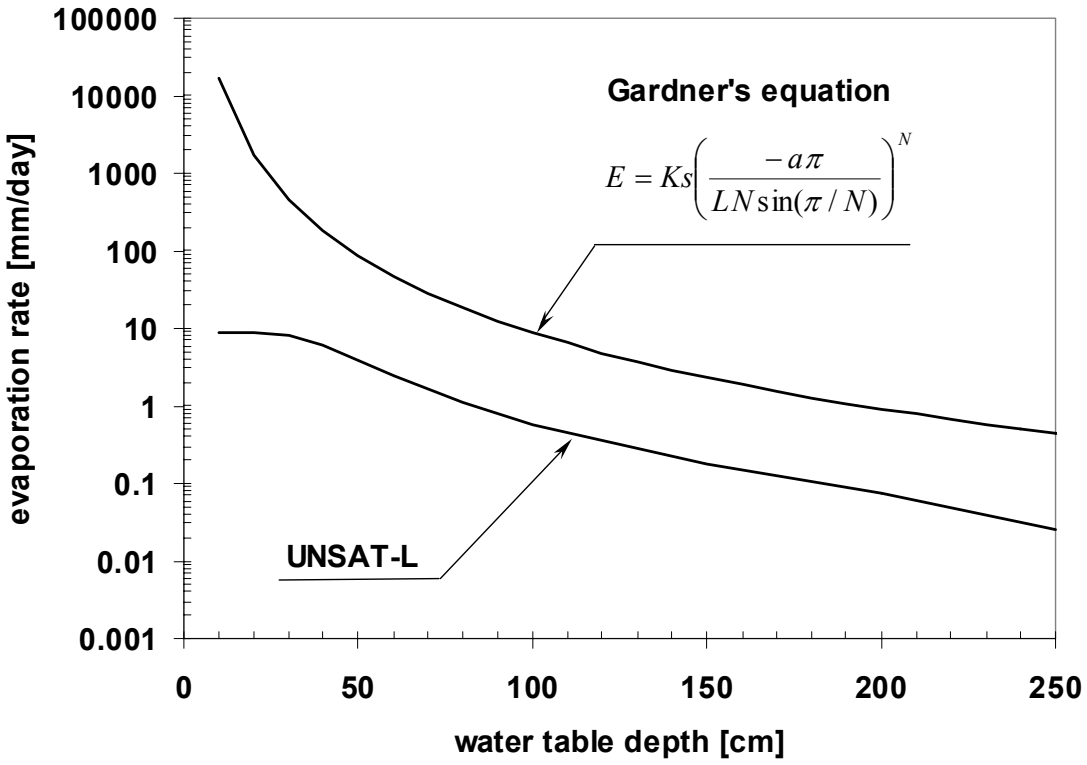

Figure 2.5 - Comparison of results from numerical simulations and Gardner's solution. Soil type was a loam. Details of calculations and soil properties are given in Appendix A.

2.2.4 Predictive function

A close-form solution to predict soil water evaporation is developed from Gardner's equation. Gardner's equation does not accurately predict the magnitude of the evaporation, but it does reasonably capture the variation in water table evaporation as a function of water table depth and soil properties. The following equation was developed to scale Gardner's equation to UNSAT-L predictions:

$$E = PETR\ e^{\chi}\ Ksat\ [(-a\pi)/(L\ N\ \sin(\pi))]^N \qquad (2.1)$$

E = evaporation rate (mm/day)
L = distance to water table (mm)
PETR = potential evapotranspiration ratio
χ = empirical scaling factor
N, a = Gardner's fitting parameters for soil hydraulic conductivity
Ksat = Saturated soil hydraulic conductivity (mm/day)

The influence of the climate on evaporation is reflected in the dimensionless potential evapotranspiration ratio, which is daily PET (mm/day) calculated by Penman's equation divided by a PET of 10 mm/day.

The value of the scaling factor varied with the soil. Figure 2.6 shows the calculated values for the parameter χ from a curve fitting equation to the different evaporation curves. An average value for χ=-3 was found to be reasonable for all of the results. If a soil-specific value for χ is not available, using χ=-3 allows a reasonable estimate of water table evaporation to be calculated from a single equation with only readily determined soil parameters, PET, and water table depth.

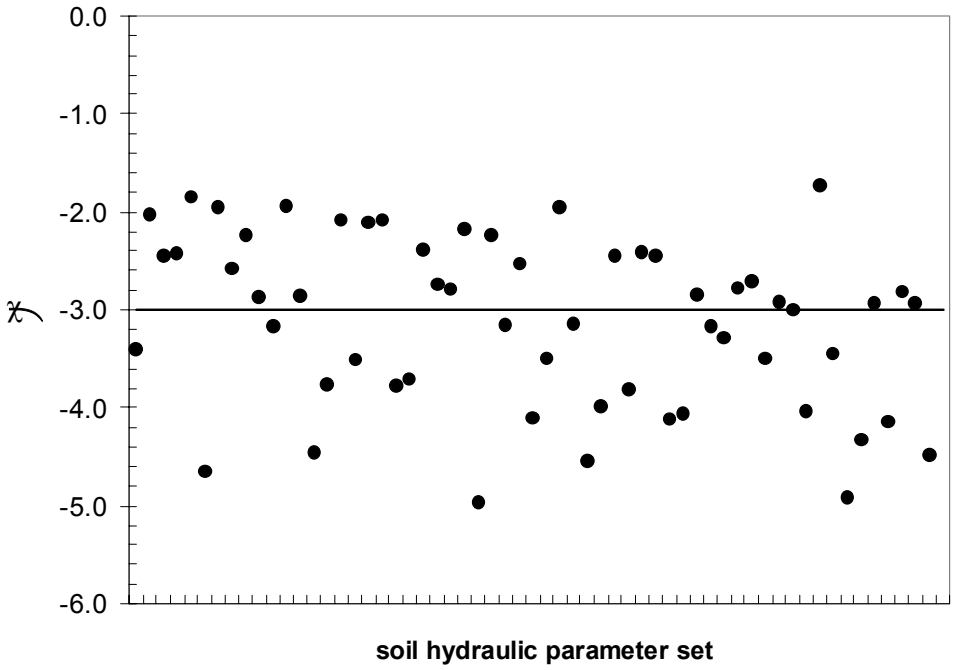

Figure 2.6 – Variation in the evaporation scaling factor χ for simulations with different hydraulic properties. Details of calculations are given in Appendix A.

Figure 2.7 shows the evaporation calculated by UNSAT-L for loam along the adjusted values for Equation 2.1 using χ=-3 and PET=10 mm/day. The maximum possible evaporation rate approaches PET; this upper bound was found to be best represented by 0.85 PET.

The predictive equation for water table evaporation is therefore given as

$$E = \text{Min}\left(PETR\, e^{\chi}\, Ksat\, [(-a\,\pi)/(L\,N\sin(\pi))]^{N},\ 0.85\ PET\right) \qquad (2.2)$$

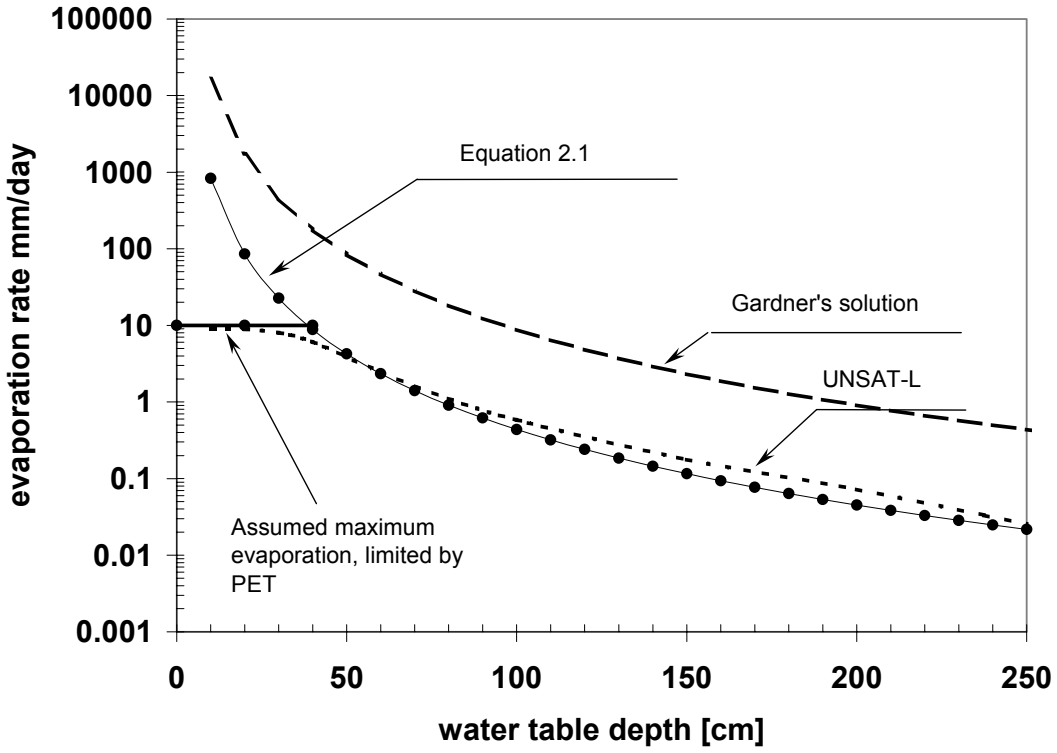

Figure 2.7 – Comparison of evaporation from numerical simulation (UNSAT-L) and Equation 2.1, and Gardner's solution. Soil type was loam. Details of calculation are found in Appendix A.

2.2.5 Soil parameters for water table evaporation model

The water table evaporation model was developed based on simulations of over 20 different soils. The properties of these soils are given in Appendix A, along with the calculated steady-state water table evaporation rates. The soil properties database given in Appendix A was developed from published soil hydraulic properties. This database and the calculated steady-state evaporation rates reveal that a wide range of hydraulic properties, and consequently water table evaporation rates, were obtained for soils with the same textural classification. Thus, it is not possible to meaningfully assign a single set of properties to represent a soil type (e.g. sand, silt loam, etc.).

2.3 Total soil water evaporation model

2.3.1 Introduction

A predictive model that includes transient evaporation in addition to water table evaporation was developed by modifying an existing water balance type model. The FAO-56 model (Allen et al., 1998) was used as the basis for this model because

1. The FAO-56 method is widely used, and there is considerable published information about its implementation for agricultural applications,
2. The method has been used to predict bare soil evaporation with reasonable results (Allen et al., 2005; Mutziger et al., 2005),
3. The method includes an explicit yet simple dependence of evaporation on water content,
4. Climate data input requirements are consistent with what is typically available,
5. The Penman-Monteith method is used as reference ET, which is widely accepted method,
6. The method can be implemented within a simple water balance approach in a spreadsheet or simple program, and
7. The method can be expanded to include vegetation (which is its principal application by others).

The FAO-56 method does not have the capability to model water table evaporation. This feature was added to the FAO-56 method as part of this study.

2.3.2 Transient evaporation model implemented in FAO56

2.3.2.1 Summary of FAO-56

The FAO-56 method is used to calculate evapotranspiration (Allen et al., 1998). The method utilized here is referred to as the "dual crop" version of the FAO-56 method, referring to the explicitly separate consideration of root zone evapotranspiration and evaporation from the soil surface. For the application considered here, the transpiration portion of the method is not utilized; all evapotranspiration is evaporation.

The ET processes occur within a root zone, which extends from the ground surface to the root depth extent. A thin surface layer is included as a subset of the root zone. As part of the ET calculation, it is necessary to have a daily accounting of the water in both the surface layer and the root zone. Soil water evaporation occurs from the bare soil surface as well as from the root zone via “diffuse” evaporation from deeper portions of the soil.

Evaporation from both the soil surface and from deeper within the root zone are calculated as proportional to a reference evapotranspiration (ET_0). ET_0 is the hypothetical ET from a surface with a stand of reference vegetation (grass or alfalfa) under optimal conditions (e.g., not short of water) and subjected to the climatic conditions of the location of interest. The calculation of ET_0 includes air temperature, relative humidity and wind speed, and serves as a measure of the atmospheric demand for water for a specific location and time.

The actual evapotranspiration is, in general, different than the reference evapotranspiration. A principal cause of the difference between actual and reference evapotranspiration is that the actual vegetation at the location of interest will not be the same as the reference vegetation. To account for the specific vegetation, a basal

transpiration or crop coefficient (K_{cb}) is used. The transpiration coefficient varies throughout the year to reflect the variation in evapotranspiration expected over the course of a year, including dormant periods when the vegetation does not transpire. A non-zero transpiration coefficient during dormant periods or in the absence of vegetation can account for "diffuse evaporation" from deeper portions of the root zone beneath the evaporative node. This is the interpretation of the basal transpiration coefficient for our application of bare soil evaporation.

The basal transpiration coefficient is applicable to optimal conditions and does not include stress due to water shortage or other factors that would limit the amount of evapotranspiraton. This evapotranspiration is referred to as evapotranspiration under standard conditions. A water stress coefficient (K_s) is used to account for the influence of the water stress on evapotranspiration. The water stress coefficient is calculated based on the characteristics of the vegetation and the amount of water in the root zone, and ranges from 1 when there is no water stress to 0 when evapotranspiration completely shut down due to a lack of water. Evapotranspiration under non-standard conditions, then, is given by the general equation

$$\text{Evapotranspiration} = K_s * K_{cb} * ET_0 \qquad (2.3)$$

Evaporation is assumed to occur from the portion of the surface that is exposed to solar radiation and precipitation, which is synonymous with bare soil that is not beneath a canopy. An evaporation coefficient (K_e) is calculated from the energy available for evapotranspiration and the transpiration coefficient, ensuring that evaporation and transpiration combined do not exceed the amount of available energy for these processes. An evaporation reduction factor (K_r) is used to account for the decrease in evaporation as the soil surface dries. At a value of K_r =1, evaporation occurs at the maximum rate associated with a wet soil surface; at a value of K_r = 0, the soil surface has dried sufficiently to result in no evaporation. The general equation for evaporation is given as

$$\text{Evaporation} = K_r * K_e * ET_0 \qquad (2.4)$$

2.3.2.2 Calibration of FAO-56 method

An energy balance experiment was established in the spring of 2005 at the CE Bosque Laboratory (10 acres adopted from the City of Albuquerque Open Space Division), which is located north of the Central Bridge on the west side of the Rio Grande. This experiment includes a sub-surface load cell based lysimeter to measure evaporative losses from the soil. The lysimeter was housed in a wooden box buried at the experiment site. The housing was fitted with an acrylic sleeve, allowing the surface of the ambient sample to sit at the same height as the surrounding soil. Instrumentation allowed for the collection of net radiation (R_n), soil heat flux (G), and sensible heat flux (H). In addition, a weather station was located on site to collect precipitation data, air temperature and humidity, and wind speed. A photograph of this experiment is shown in Figure 2.8. Data collection and analysis began at this site in April 2005 and concluded in early 2007. There were months of continuous data collection with intermittent periods of equipment malfunction precluding data collection. Complete details about the

experimental setup can be found elsewhere (Appendix B, Stormont et al., 2006).

Figure 2.8 - Simplified soil-surface energy balance experiment located in the riparian zone along the Rio Grande in Albuquerque, NM.

The FAO-56 method was calibrated to data from March 23 to August 22, 2005. The calibrated model was then used to make a forward prediction for comparison of data collected from November 18, 2005 to September 26, 2006 to evaluate the robustness of the model. The calibration of the FAO-56 method to data from this experiment is explained in more detail in Appendix B. A brief summary is presented here.

It was necessary to modify the FAO-56 method in order to be applicable to the lysimeter. Because there is a bottom on the lysimeter, the water content within the lysimeter can exceed field capacity that is not permitted in the conventional FAO56 method. To accommodate the lysimeter, the amount of water in the lysimeter was allowed to exceed the field capacity by permitting the depletion to be a negative number, limited by the porosity of the soil.

The first step in the calibration was to interpret evaporation from the lysimeter data. On days without rain, the evaporation was simply the loss in mass as measured by the lysimeter. On days that it rained, it was necessary to add the weight of rain to the change in lysimeter mass to have a net measure of evaporation for the day.

Another adjustment of the lysimeter data was necessary to account for the days where the rainfall was so intense that there was surface run-off. For the first 4 mm of rainfall, no runoff was observed, and most or all rainfall infiltrated into the soil. This is consistent with typical infiltration behavior, in which rainfall initially infiltrates fully until the surface wets and runoff begins. For each day with a precipitation of greater than 4 mm, the 15-minute lysimeter output and precipitation values of that day were tabulated. Runoff was calculated as the precipitation at a time during a storm minus the lysimeter response to the precipitation. The method assumes that during the 15-minute period with rain, the lysimeter did not lose any water by evaporation. The sum of these differences was calculated and taken to be the day's runoff.

Finally, on a few days, the interpreted evaporation from lysimeter data significantly exceeded the potential evapotranspiration. These days were associated with very high rainfalls, suggesting the method of adjusting for run-off may have been inadequate for those conditions. On these days, the maximum evaporation rate was constrained to no greater than the potential evaporation calculated using Penman's equation for open water conditions.

The calibration of the FAO-56 method involved adjusting the surface layer thickness, Z_e, and two parameters related to the diffuse evaporation from the root zone, p and K_{cbmin}. The remaining input values were either measured or taken from published recommended values. The surface layer thickness is generally recommended to be in the range of 0.1 and 0.15 m (Allen et al., 1998). The thickness of the layer controls in part how much water is held in the surface layer and available for surface layer evaporation. The p parameter is used in the calculation of the water stress parameter Ks. The value of p is related to the decrease in transpiration as soil dries out, and varies from a maximum of 1, where there is no decrease in transpiration with decreasing water content, to 0, where the transpiration rate decreases immediately as the water content decreases below field capacity. The value of p is most often taken as 0.5 (Allen et al., 1998). There is no published guidance for a value for p appropriate for bare soil evaporation. Kcbmin for bare soil is suggested to vary from 0 to 0.20 (Allen et al., 1998). Generally, the drier the soil gets, and the lower K_{cbmin} is expected. For soils that experience dry conditions over long times, K_{cbmin} has been recommended to be 0 (Allen et al., 1998).

The best fit to the 2005 data was achieved with a surface layer thickness of 0.15 m, p=0.999, and K_{cbmin} = 0.09. A comparison of the FAO-56 method with these values and the experimental data from 2005 is shown in Figure 2.9. With these parameters, the FAO-56 method predicted evaporation reasonably reproduces the magnitude and character of the measured evaporation. The rapid loss of water in the surface layer in response to precipitation events can be seen clearly in the measured and predicted response. Between the large evaporation rates in response to precipitation events, the measured response shows a lower evaporation rate. The FAO-56 response simulates this behavior through the diffuse evaporation component, but not always at the rate as that measured. The diffuse evaporation rate is directly related to both p and K_{cbmin}. The value of K_{cbmin} is in the expected range. The value of p is at the upper end of allowable values, and exceeds the usual upper limit of 0.8 (Allen et al., 1998). The large value of p

indicates that the diffuse evaporation rate will be constant until the soil dries to the total available water limit. This result may occur because the evaporation is actually controlled by vapor phase diffusion from within the soil to the atmosphere, causing an essentially constant rate as long as there is some available water in the soil. On the other hand, this result seems counter to the process of water having to move from lower to upper regions in the soil in order to be evaporated, which would be expected to be a function of water content. FAO-56 guidance suggests that K_{cbmin} decreases as the soil dries. It may be that this somewhat counter-intuitive result obtained here is a consequence of calibrating the model with data from a shallow lysimeter, which limits how far water has to move until it can be evaporated.

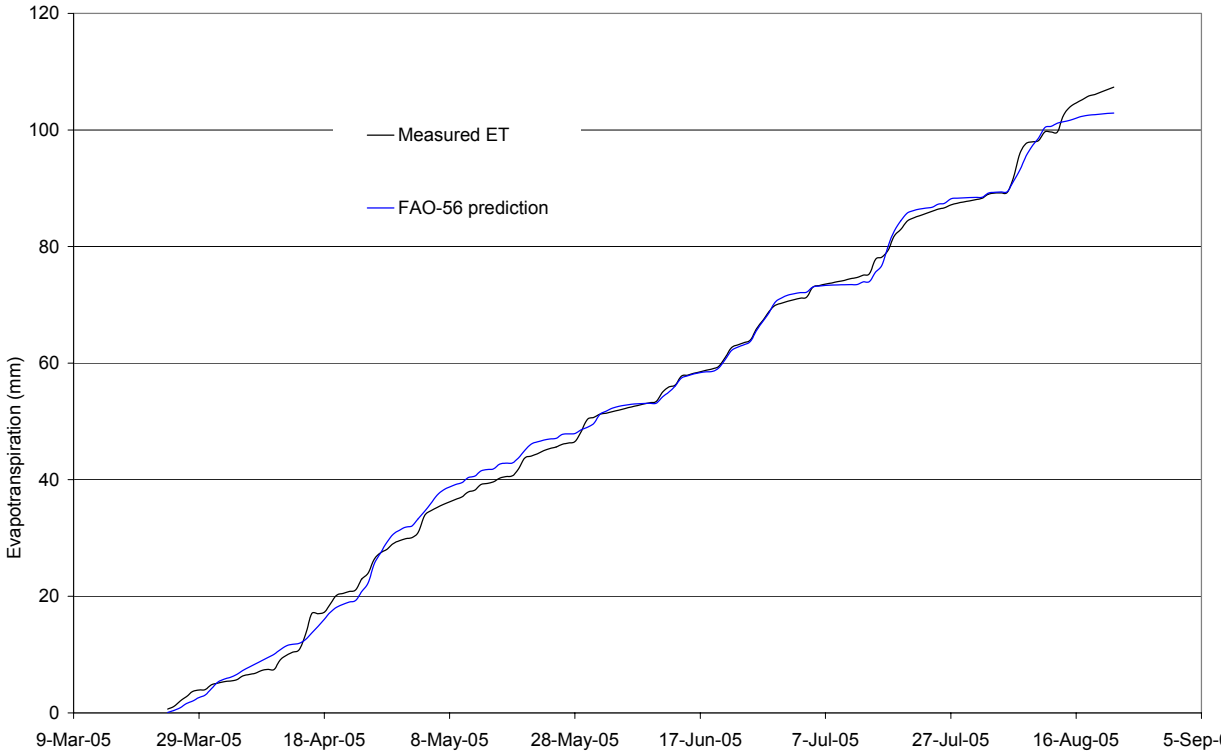

Figure 2.9 – Measured evaporation and calibrated FAO-56 predicted evaporation for location in Middle Rio Grande valley. Details are given in Appendix B.

The FAO-56 method with the calibrated values was then applied to the 2006 data set without any further adjustment. As shown in Figure 2.10, there is reasonable agreement between the measured and FAO-56 method predicted values, suggesting the robust nature of the FAO-56 method. This result is especially significant because these data cover a long time period, and includes many large precipitation events and corresponding large daily values of evaporation. These results confirm the ability of the FAO-56 method to serve as a practical method to reasonably estimate soil water evaporation in the Middle Rio Grande region.

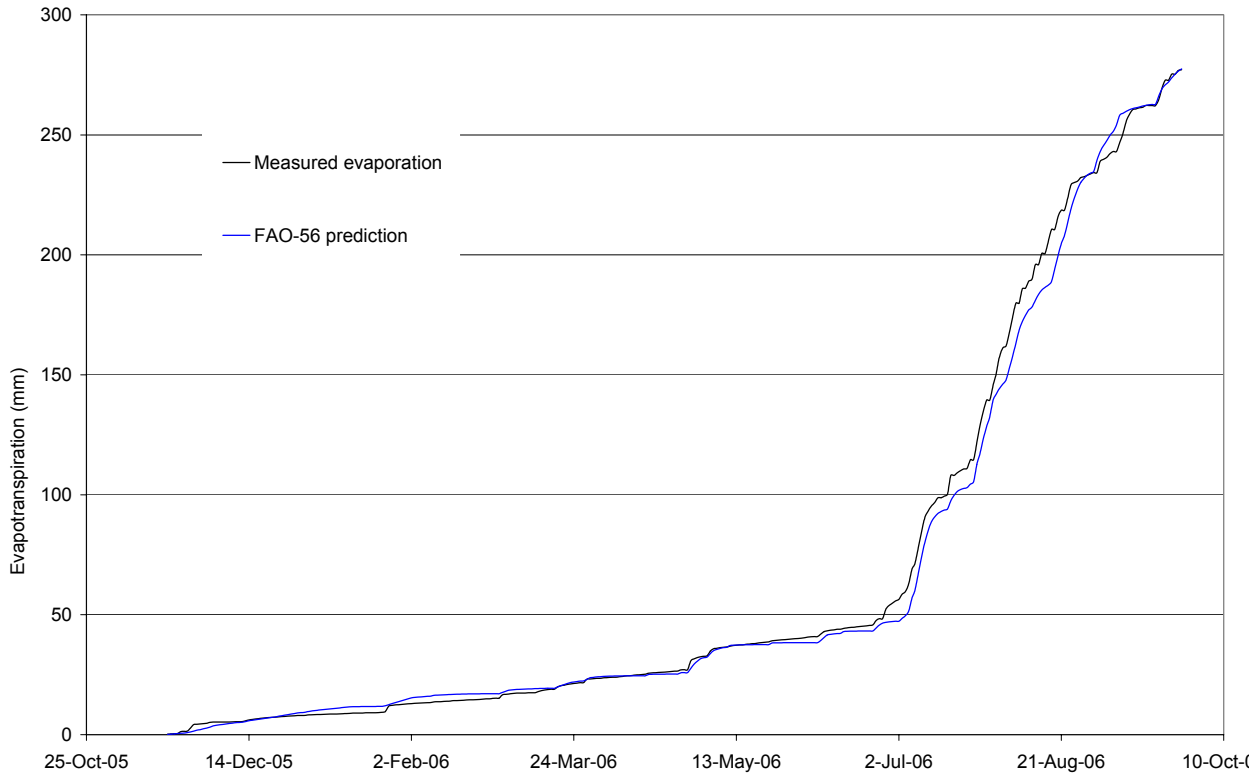

Figure 2.10 – Forward predicted evaporation using the calibrated FAO-56 method and measured evaporations at location in the Middle Rio Grande Valley. Details are given in Appendix B.

2.3.3 Modifications to FAO-56 method

2.3.3.1 Incorporating water table evaporation into the FAO-56 method

The water table evaporation function previously developed (Equation 2.2) was incorporated into the FAO-56 method. With this modification, the amount of water evaporated from a shallow water table is included in the daily estimates of ET. The water table evaporation was added as an additional component, so the computation of the surface layer evaporation and diffuse evaporation were not modified.

2.3.3.1.1 Additional soil properties to input

In order to implement this equation into the FAO-56 method, additional unsaturated hydraulic properties are required. These properties include parameters for Gardner's conductivity function (Jury et al., 1991), the saturated hydraulic conductivity, and the water table evaporation function scaling factor.

2.3.3.1.2 Water table distance input

The method allows the water table to vary on a daily basis to accommodate changing river stages or some other process that would affect the water table. Therefore, an estimated or assumed water table depth is a required input for every day.

2.3.3.1.3 Daily Penman calculation

The water table evaporation function uses Penman's PET equation to account for atmospheric demand for water. Penman's PET can be calculated from the daily climatic input used to calculate reference evapotranspiration in the FAO56 method.

2.3.3.1.4 Initial water in the root zone

One of the necessary modifications to the FAO-56 method concerns the amount of water in the root zone due to a shallow water table. The amount of water in the root zone is important because it affects the available storage as well as the water stress factors for calculating ET. The initial amount of water in the root zone associated with a shallow water table depth was based on the results of the steady-state water table evaporation calculations using UNSAT-L. For each soil type, the amount of water in the top 1 m (the thickness of the root zone used here) was calculated for distances to the water table between 100 mm and 2.5 m. These values were fit to a 2^{nd} order polynomial, and used to estimate the water in the root zone for water table distances to 2.5 m. Beyond 2.5 m, the initial amount of water in the root zone due to the water table was assumed to decrease linearly to zero at 5 m. The amount of water in the root zone will change if the distance to the water table changes.

2.3.3.1.5 Modification to minimum depletion in root zone

When the water table is close to the surface, the amount of water in the root zone can exceed the field capacity. However, the FAO-56 method does not allow for water contents above field capacity. Therefore, FAO-56 was modified to allow for negative depletion equivalent to the amount of water in the root zone from the calculation described above.

2.3.3.1.6 Maximum water table evaporation

The daily maximum amount of water table evaporation (E_{wtmax})is found by implementing the relationship derived from the numerical simulations (Equation 2.2). This evaporation rate can be calculated from the soil properties, the distance to the water table, and the atmospheric demand for water as follows:

$$E_{wtmax} = \text{Min} (B * G * A * ET_0, 0.85 * A * ET_0) \qquad (2.5)$$

where

$G = K_{sat} [(- a \pi)/(L N \sin(\pi))]^N$ (mm/day)

$A = PETR/ET_o$

$B = e^{\chi}$

2.3.3.1.7 Limits on water table evaporation

Because it is possible there is a limited amount of energy available to evaporate soil water, it may be that E_{wt} will be less than the maximum value. The energy has to be partitioned into consumption by the root zone in the traditional sense (via K_{cb}), the surface layer (via K_e) and the water in the root zone from the water table (via K_{wt}). K_{wt} is a new term that we are introducing to the FAO-56 method.

The values of K_{cbmax} and K_e are calculated in the usual way following the FAO-56 methodology. K_{cb} is fixed at K_{cbmin} for the cases without vegetation. K_{wt} is calculated as

$$K_{wt} = \text{Min} [E_{wtmax}, (K_{cmax} - K_{cb} - K_e)] \quad (2.6)$$

K_{wt} is constrained to be equal or greater than zero.

With this approach, the surface layer and the diffuse evaporation occur first. The remaining energy is then available for water table evaporation. The rationale for this approach is that water in the surface layer will evaporate first. This approach also minimizes modifications to existing FAO-56 method.

2.3.3.1.8 Total ET

Finally, the general ET formula for total soil water evaporation is

$$ET = (K_s K_{cbmin} + K_e + K_{wt}) ET_0 \quad (2.7)$$

The water table evaporation is $K_{wt} * ET_0$.

2.3.3.1.9 Capillary rise

When there is a shallow water table, it is necessary to account for capillary rise from the water table in response to a loss of water from ET. The capillary rise is taken as the amount of ET from water table evaporation and the diffuse evaporation

$$\text{Capillary rise} = (K_s K_{cbmin} + K_{wt}) ET_0 \quad (2.8)$$

Adding this amount of water to the root zone to represent daily capillary rise will keep the water content of the root zone largely constant from day to day. The water in the surface layer is not adjusted based on capillary rise as it is principally intended to account

for transient evaporation due to precipitation.

2.3.3.2 Incorporating a shade model into FAO-56

A shade model was incorporated into the FAO-56 method in order to account for the impact of shade on the amount of bare soil water evaporation. For the applications of concern here, shade is assumed to be from a tree canopy. The shade calculation is related to the fraction of ground cover term in FAO-56, but uses different input (e.g., LAI in this method vs. crop coefficients in FAO-56).

The conceptual shade model is shown in Figure 2.11 below. Some direct sunlight penetrates the canopy and reaches the soil surface, whereas the remainder of the soil surface is in the shadow of the canopy. The portion of soil in direct sunlight will receive both direct (or beam) solar radiation, Sb, and diffuse radiation, Sd. Diffuse radiation arises from scattering from the atmosphere. In the canopy shadow, the soil surface only sees diffuse radiation.

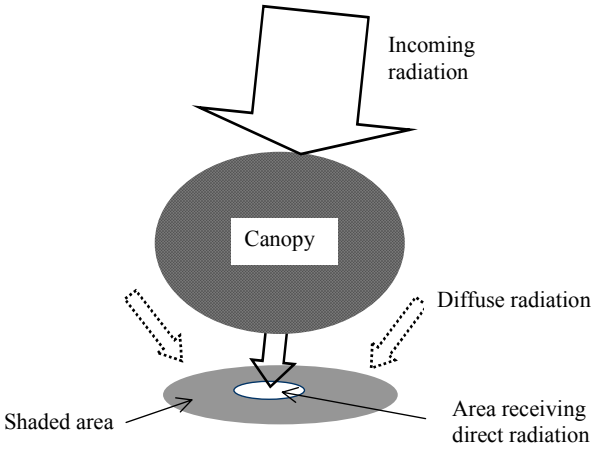

Figure 2.11 - Conceptual model of shade beneath canopy.

The total radiation per unit area (S_{ts}) is estimated from the fraction area average of the portion of the soil that receives direct sunlight and that which is in the shadow of the canopy.

$$S_{ts} = (S_b + S_d) * A + S_d * (1-A) \qquad (2.9)$$

where A is the fractional area that receives direct sunlight. This equation can be expressed as the ratio of the solar radiation with shade (S_{ts}) to that without shade (S_t)

$$S_{tsfrac} = S_{ts}/S_t = A + (S_d/S_t) * (1-A) \quad (2.10)$$

2.3.3.2.1 Estimate of area that receives direct sunlight

The fraction of incident sunlight that penetrates a canopy is (Campbell and Norman, 1998)

$$A = \exp(-K_b(\psi) * LAI) \qquad (2.11)$$

where ψ is the zenith angle of the sun, which is the angle the sun measured from the vertical; $K_b(\psi)$ is the extinction coefficient, which is the fraction of the leaf surface area that is projected onto a horizontal plane as a function of ψ; and LAI is the leaf area index, which is the one-sided area of leaf surfaces per unit area.

The leaf area index can be expressed as a function of the day of year. One simple approach is to assume that there is a day of the year on which leaves begin to grow and the LAI becomes non-zero. The LAI increases linearly as the leaves grow until the maximum LAI is reached. The LAI remains at the maximum value until it decreases linearly to eventually reach zero.

The zenith angle varies as a function of the solar declination, latitude, and time of day relative to solar noon. The zenith angle was determined for each hour of each day for Albuquerque, NM using Equations 11.1, 11.2, 11.3, and 11.4 of Campbell and Norman (1998).

The extinction coefficient was calculated during daylight hours from (Campbell and Norman, 1998)

$$K_b(\psi) = (2*\cos(\psi))^{-1} \qquad (2.12)$$

This equation assumes that the leaf angle distribution is spherical, which is considered a reasonable approximation for many canopies (Campbell and Norman, 1998). There are other equations applicable to other leaf angle distributions that could be implemented if desired.

For each hour of sunlight for a given day, the fractional area that receives direct sunlight can be calculated from Equation 2.11 using the hourly extinction coefficients and daily LAI values. An average value for each day is then calculated.

2.3.3.2.2 Estimate of diffuse radiation in shadowed areas

The ratio of diffuse to total solar radiation can be found by simultaneously solving equations 11.9, 11.8, 11.11 and 11.13 from Campbell and Norman (1998) to yield

$$S_d/S_t = [(0.3 * (1- \tau^m)) / \tau^m] \qquad (2.13)$$

where τ is the atmospheric transmittance and is assumed to equal 0.7 as typical of a clear day (Campbell and Norman, 1998). M is the optical mass number and is a function of the

atmospheric pressure and zenith angle. It is calculated from Equation 11.12 (Campbell and Norman, 1998).

For each hour of sunlight for a given day, the ratio of diffuse to total solar radiation is calculated from Equation 2.13 using the hourly optical mass numbers. An average value for each day is then calculated.

2.3.3.2.3 Net radiation beneath canopy

The ratio of the solar radiation with shade (S_{ts}) to that without shade (S_t) is found by substituting the average daily values for the area that receives direct sunlight and the diffuse to total solar radiation ratio into Equation 2.10.

The calculation is only for incident solar radiation. Net radiation includes accounting for reflected shortwave radiation (albedo) and longwave radiation. Albedo is a function of the surface, and is assumed to not vary significantly as a function of canopy shading. The longwave radiation depends on the surface temperature of the soil. Shaded areas are cooler and there would be less longwave radiation, but there is no attempt here to quantify the soil temperature or longwave radiation differences. For simplicity, it is assumed that the longwave radiation is affected proportionally to the shortwave radiation. In the case, the net radiation is given as

$$R_{netshade} = R_n * S_{tfrac} \qquad (2.14)$$

where R_n is the net radiation in the absence of shade as calculated by the FAO-56 method.

An example for the calculation of S_{tfrac} is shown in Figure 2.12. Prior to the onset of growing season on day 90 and after senescence on day 310, the soil beneath a canopy receives full sunlight and the net radiation is not diminished. When there are leaves, the canopy intercepts a portion of the incident radiation and the soil surface sees less net radiation. Even in full shade (with about 1% direct sunlight for this case of a maximum LAI of 4), the soil will experience net radiation due to the diffuse component of radiation.

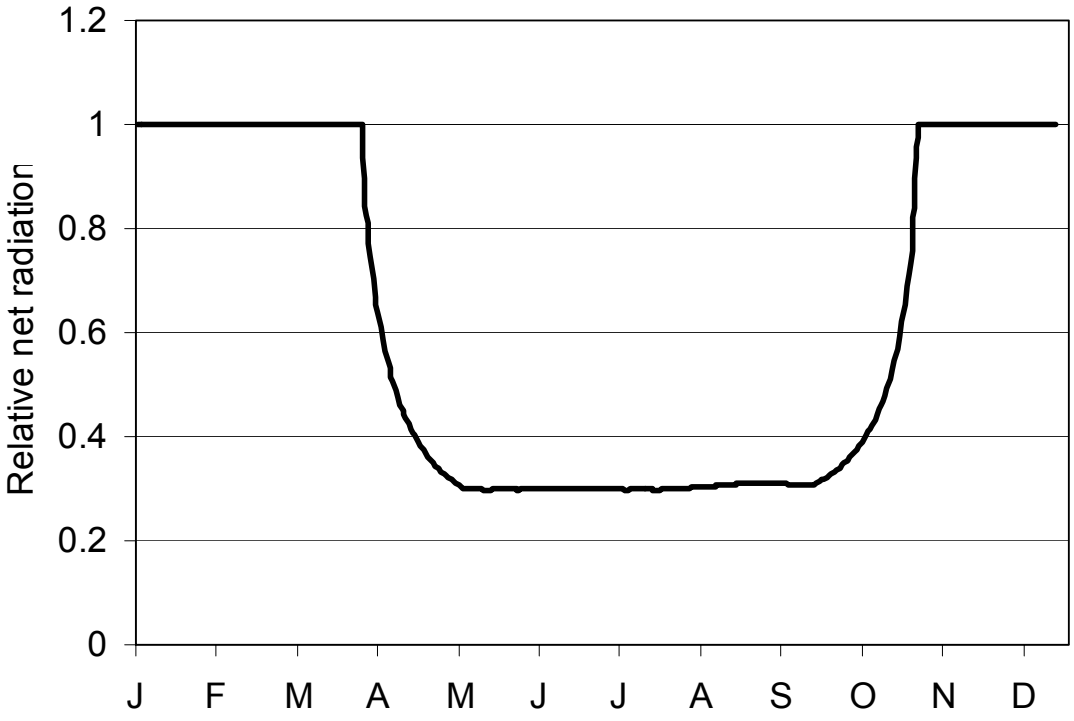

Figure 2.12 - Relative net radiation beneath cottonwood canopy.

2.3.3.3 Incorporating surface mulch into FAO56

Surface mulch is a surface layer with an open structure relative to typical soils. The mulch can be organic (e.g., bark) or soil (e.g., gravel). Mulch limits evaporation because of its open pore structure: at any condition except saturation, large open pores are largely impermeable to water. Thus, mulch severely limits the transport of liquid water to the surface for evaporation.

The FAO-56 method can simulate mulch if the surface layer is assigned the properties of a very coarse soil. In this way, infiltration through the surface layer will occur rapidly due to the very low field capacity of this layer. Any water that remains in the surface layer can evaporate.

When water table evaporation is considered in a case with mulch, it will be necessary to assign the water table evaporation parameters to those of a very coarse soil and not those of the root zone. However, the initial water content calculation for a shallow water table should be based on the properties of the root zone soil. Thus, the soil properties for both sets of soils must be known.

3 Application of total soil water evaporation model

The total soil water evaporation model described in Chapter 2 was implemented into a spreadsheet. This model is a modified version of the FAO-56 method that explicitly includes water table evaporation. The model was applied to a location in the Middle Rio Grande bosque to demonstrate its use and to provide insight into how soil water evaporation may be impacted by restoration and management activities.

3.1 Model inputs

The model was used to estimate daily soil water evaporation for the 2006 calendar year. The location used for the application of the model is a monitoring well near the Albuquerque drinking water diversion dam between the Alameda and Paseo Del Norte bridges. The well is one of many that are monitored by the Bosque Ecological Monitoring Program, and is referred to as the Minnow east well. It is located approximately 10 m from the river.

Weather data for the calendar year 2006 were obtained from a weather station adjacent to the bosque near the Albuquerque Country Club. Data from this site were selected because, in contrast to data from some of the other weather stations near the bosque, there was a continuous dataset for the entire year. Daily data required for the model to calculate reference evapotranspiration are maximum and minimum temperature, solar radiation, relative humidity, and wind speed. The calculated daily reference evapotranspiration using these data is shown in Figure 3.1.

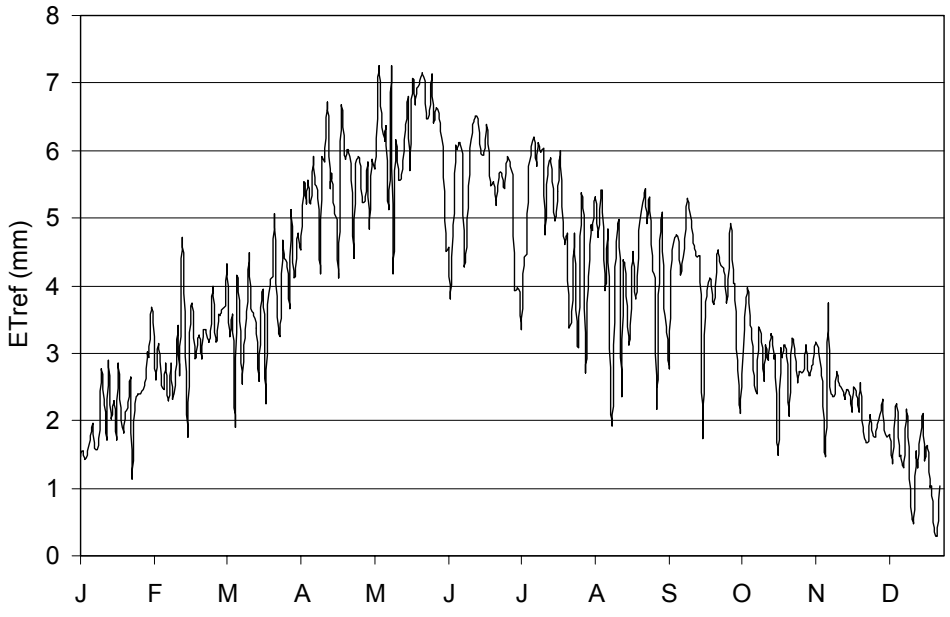

Figure 3.1 – Daily reference evapotranspiration used in total soil water evaporation model applications (2006).

The daily precipitation from the weather dataset is shown in Figure 3.2. The precipitation reveals a dry first half of the year, followed by relatively large and frequent rains during the mid-summer months.

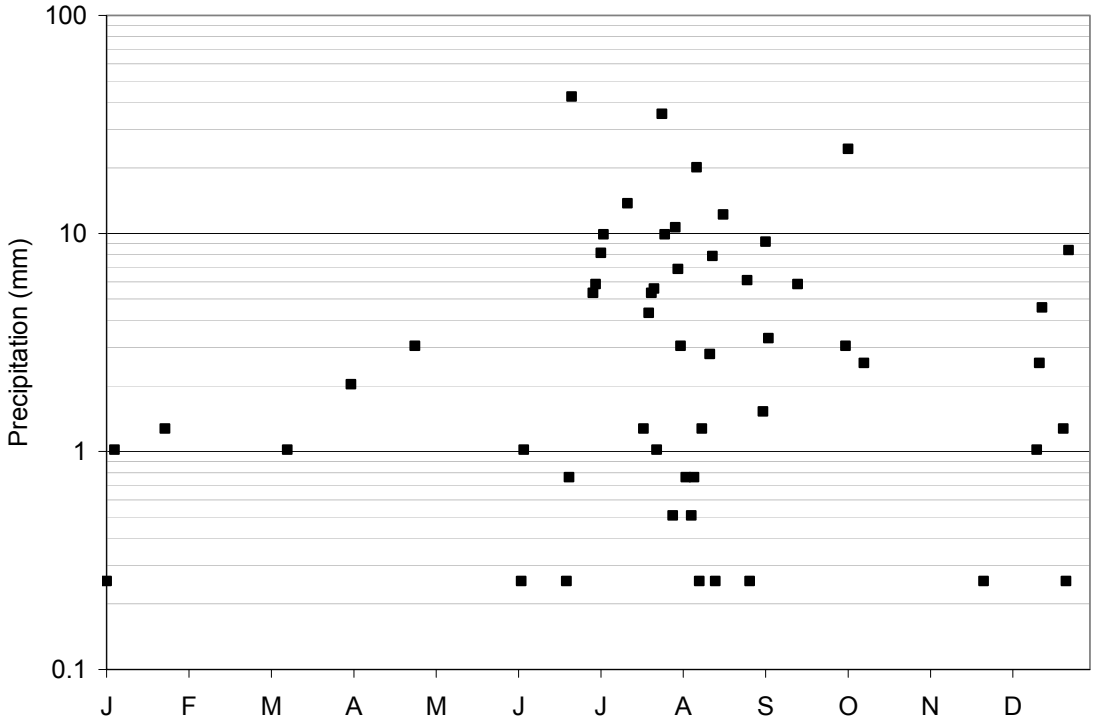

Figure 3.2 – Precipitation data used for total soil water evaporation model application (2006).

Daily water table elevations were not available from the Minnow east well for the entire 2006 calendar year. Therefore, the daily water table elevation data were derived from the relationship between the USGS Paseo del Norte gauge and the monitored water table depth in the Minnow east well (UNM, 2007). The daily water table elevations are given in Figure 3.3 below, and indicate that the water table depth is generally between 1.0 and 1.2 m at this location. A reduction of the water table in response to increased river levels during the intense summer storms of 2006 can be observed.

Characterization of the Minnow east well site reveals the soil between the ground surface and the water table is classified using the USCS method as clayey sand (UNM, 2007). In terms of the soil types that were used to develop the water table evaporation model (described further in Appendix A), this soil corresponds to loamy sand. The parameters associated with the soil used in the application of the soil water evaporation model are given in Table 3.1. This soil is referred to as the baseline soil.

Table 3.1 – Baseline soil parameters

Parameter	Description	Value
a (mm)	Constant in Gardner's function	-411
N	Constant in Gardner's function	4.62
χ	Constant in evaporation function	-2.2
FC	Field capacity	0.137
WP	Wilting point	0.064
REW (mm)	Readily evaporated water	6

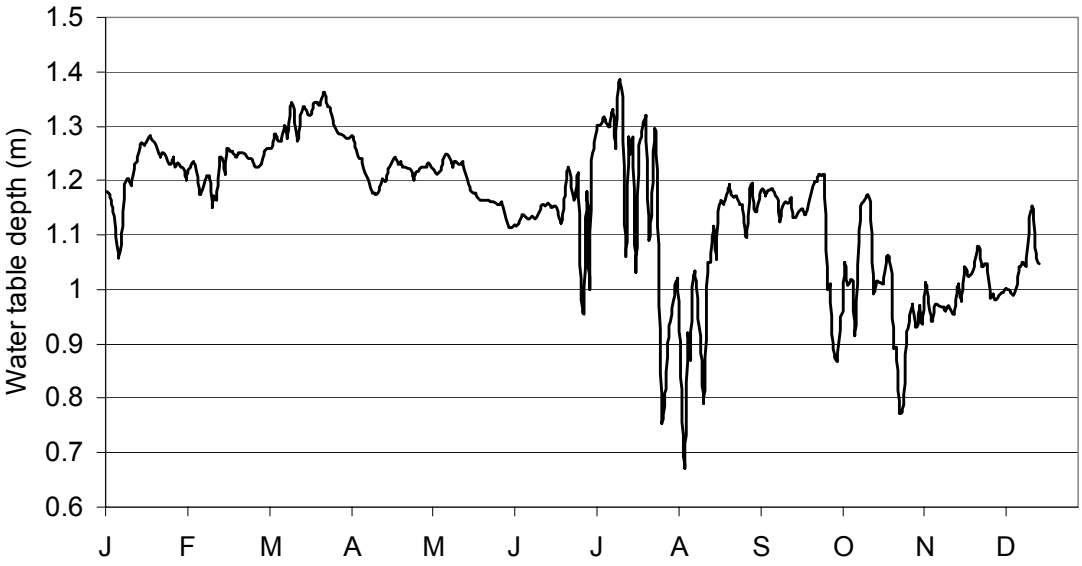

Figure 3.3 – Interpreted water table elevations at Minnow east well used for total soil water evaporation model application (2006).

Some of the model applications included considering the effects of shade on total soil water evaporation. The effect of shade was accounted for by modifying the net radiation that the soil surface is exposed to based on transmission of radiation through the canopy

(Section 2.3.3.2). For the model application, the assumption was made that the shade would be a consequence of a full cottonwood canopy. The LAI used to calculate the reduction in the net radiation was assumed to be a piece-wise linear function of the day of the year, and is given in Figure 3.4. The cottonwood LAI parameters used to estimate the shade were from McDonnell (2006).

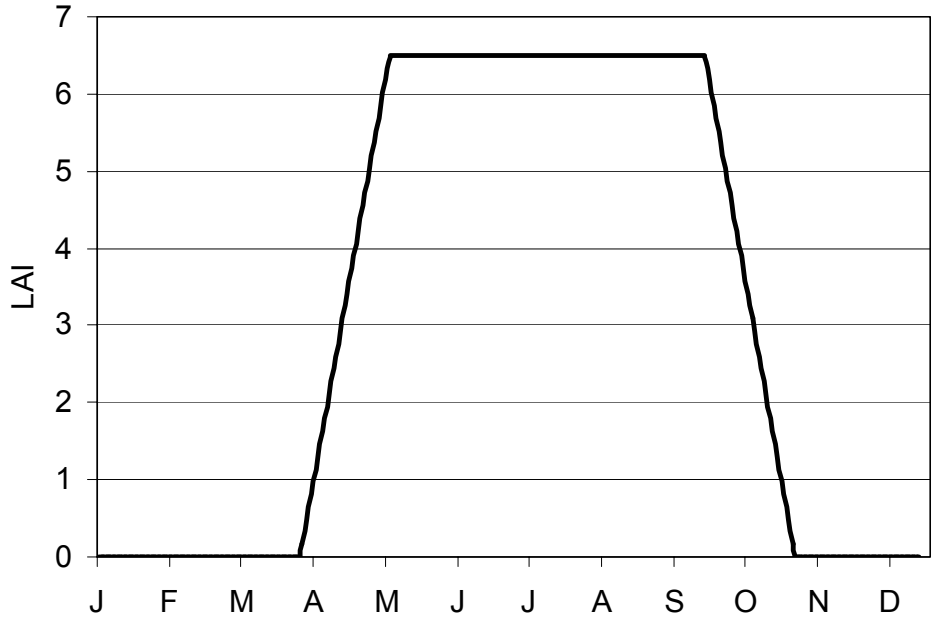

Figure 3.4 – Assumed LAI of cottonwood canopy that shades soil surface.

The reference evapotranspiration calculated using the net radiation beneath the canopy is given in Figure 3.5 below. After leaf out, there is a significant reduction in the reference evapotranspiraton (contrast to Figure 3.1). The reference evapotranspiration is reduced by more than 50% over much of the growing season.

Mulch is modeled as a thin layer of gravel on the surface. Gravel is a very coarse soil that drains quickly and becomes largely non-conducive to upward liquid water movement. This response limits water movement from within the soil profile to the surface and subsequent evaporation, and is consistent with both soil-based and organic mulches. In addition, mulch tends to reduce surface layer evaporation because it does not hold much water from precipitation before it releases it to lower portions of the soil profile. The properties and parameters of the gravel mulch were derived from the properties of pea gravel (Stormont and Anderson, 1999) and are given in Table 3.2 The mulch layer thickness was assumed to be 40 mm.

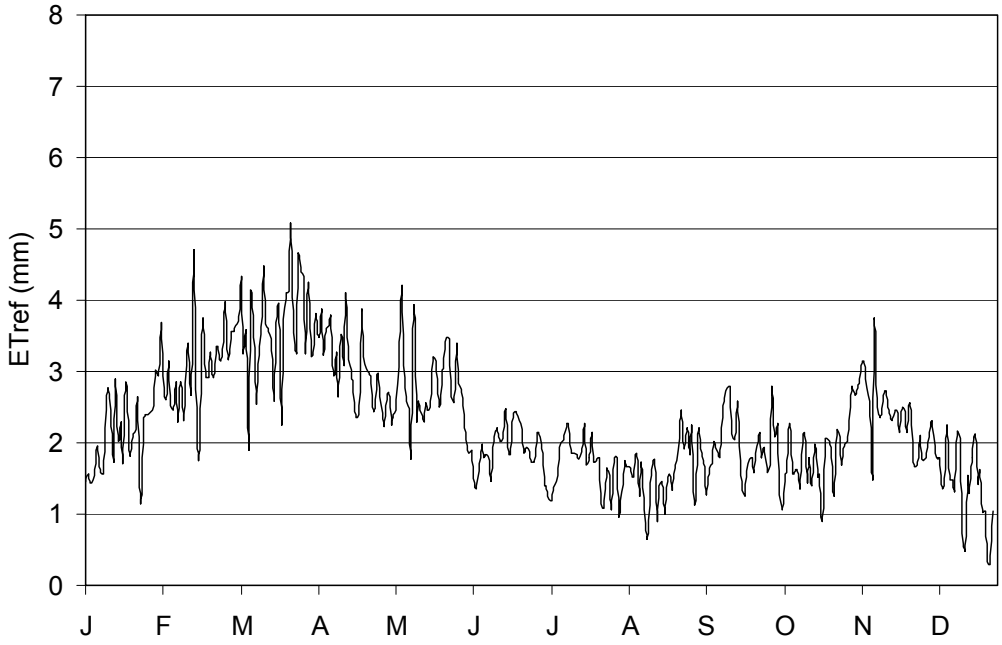

Figure 3.5 - Daily reference evapotranspiration in shade used in total soil water evaporation model applications.

Table 3.2 – Gravel mulch parameters

Parameter	Description	Value
a (mm)	Constant in Gardner's function	-4
N	Constant in Gardner's function	6.1
χ	Constant in evaporation function	-2
FC	Field capacity	0.05
WP	Wilting point	0.03
REW (mm)	Readily evaporated water	0.5

3.2 Model results

Results from the "baseline" model are given in Figure 3.6. Baseline refers to no shade, no surface mulch, and soil properties and water table elevations described previously. In addition to the components of evaporation, the reference ET is shown. During the first half of the year, when there is very little rainfall, the total evaporation is on the order of 1/3 of the reference ET. During the large precipitation events in July and August, the total evaporation often approaches the reference ET and nears its maximum permitted by the climatic conditions. During November and December, the total evaporation again approaches the reference ET due to a decrease in the water table depth and corresponding increase in water table evaporation.

The surface layer evaporation is closely correlated to precipitation events. When the surface layer wets after a rain, water in the surface layer is available to evaporate. If the surface layer gets wet enough, some of the water will move into deeper portions of the soil profile, where evaporation proceeds at a slower rate because it is controlled by diffusion. For the baseline conditions, the total annual precipitation was 310 mm, and 223 mm was lost by surface layer evaporation. This indicates that for these conditions less than 30% of the precipitation will penetrate the soil profile beyond the surface layer.

During periods when the surface layer becomes wet from precipitation such as during late summer of 2006, the water table evaporation can approach zero because the available energy goes first into evaporating water in the surface layer. When the surface soil dries out, there is significant amount of water table evaporation. This indicates a strong connection between the water table and the atmosphere as a result of a relatively shallow water table and soil properties conducive to upward water movement.

The amount of diffuse root zone evaporation is nearly constant during the year because the root zone stays at nearly constant water content from the relatively shallow water table.

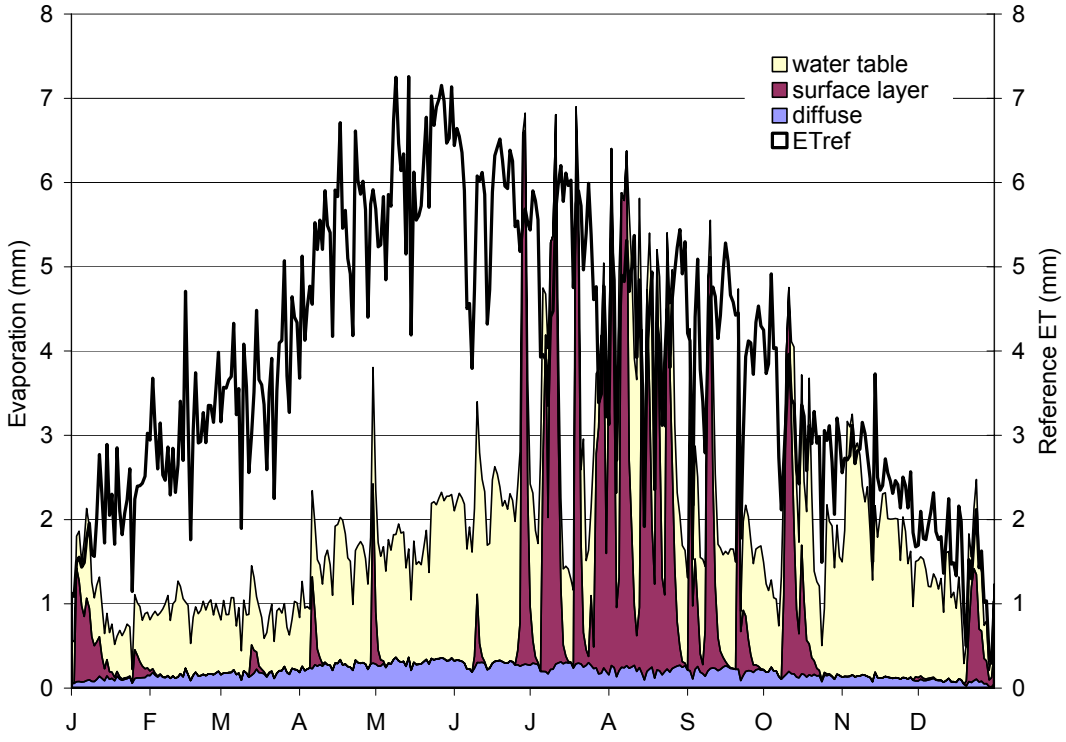

Figure 3.6 – Soil water evaporation components for baseline conditions during 2006.

When shade from a cottonwood canopy is included in the model, the effect on soil water evaporation is dramatic (Figure 3.7). The water table evaporation in early summer drops as ETref, which represents the atmospheric demand for water, begins to decrease in response to the leaf-out of the cottonwood canopy. Once the rains begin in mid-summer, evaporation is primarily from the surface layer. This is because the surface layer remains wet, as the amount that can be evaporated is less than that from previous rain. In contrast, without shade, the surface layer dried between most of the rains. During this period, there is little water table evaporation as the available energy goes first toward evaporating the surface layer water.

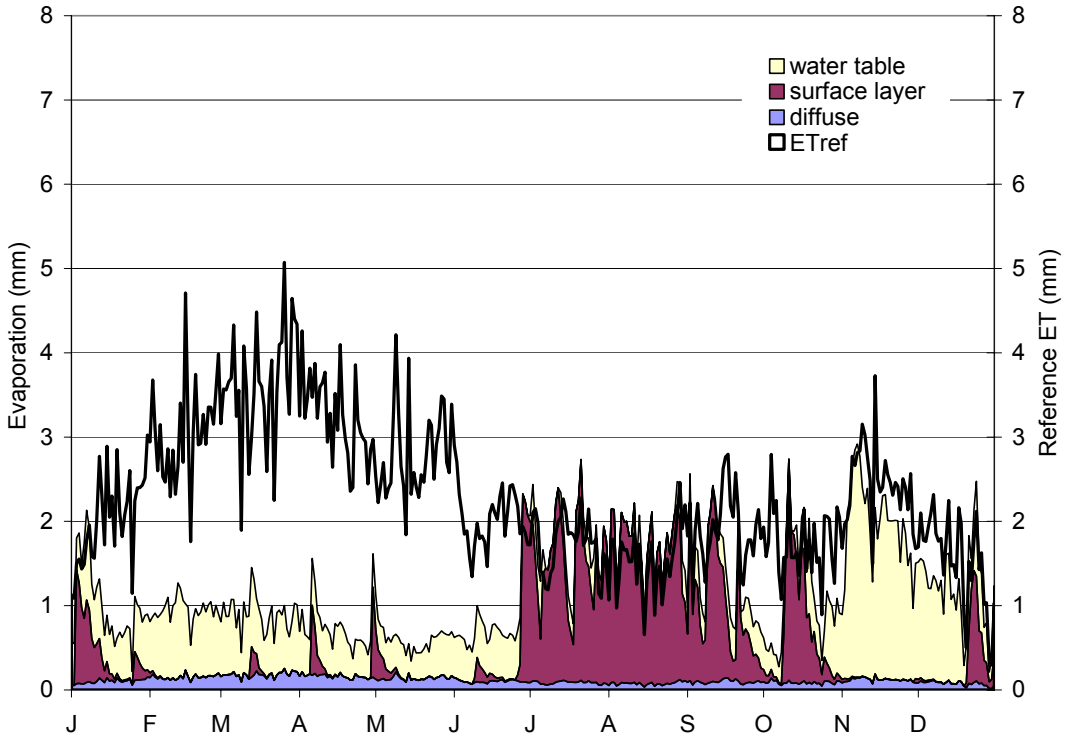

Figure 3.7 – Soil water evaporation components for baseline conditions and shade from cottonwood canopy during 2006.

Placing mulch on the surface has an even greater impact on the soil water evaporation (Figure 3.8). Because the mulch creates a barrier to upward liquid water movement at the surface, the amount of water that is lost by water table evaporation is very small. The diffuse root zone evaporation is unaffected by the mulch because it describes the relatively slow evaporation from moisture in the root zone that moves to the surface and, as implied by the name, diffuses to the atmosphere. The surface layer evaporation again responds to precipitation events, but the amount of surface layer evaporation over the course of the year is about 60% of that for the baseline conditions. Because the mulch stores less water than the loamy sand, some water will move downward into the lower portions of the soil profile before it can be evaporated.

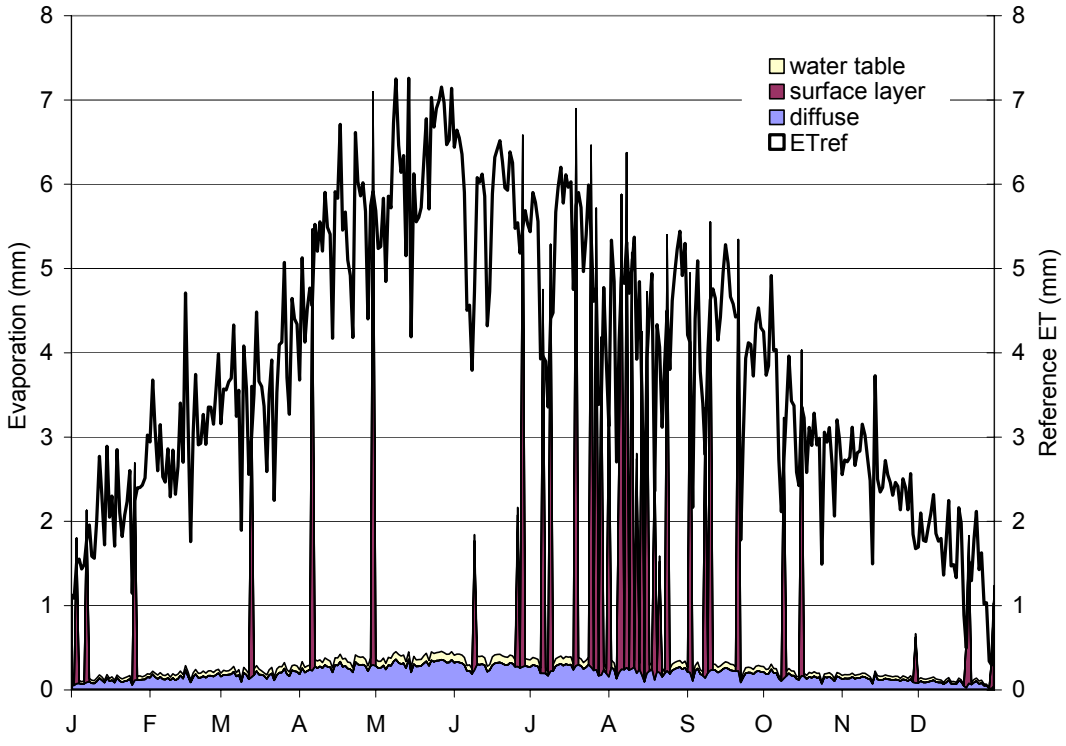

Figure 3.8 – Soil water evaporation components for baseline conditions during 2006 with a surface mulch.

A summary of the baseline results, including those with shade and mulch, are given in Figure 3.9. For a point of reference, the annual reference ET for these conditions is about 1400 mm. The baseline conditions result in an annual soil water evaporation of approximately one-half of the annual reference ET. For the baseline conditions, the water table evaporation is significant, accounting for 55% of the annual evaporation. The shade reduces the driving force for evaporation, and all of the evaporation components are diminished compared to the baseline conditions. Mulch limits the amount of water that can be drawn up to the surface and evaporated, and consequently dramatically reduces water table evaporation.

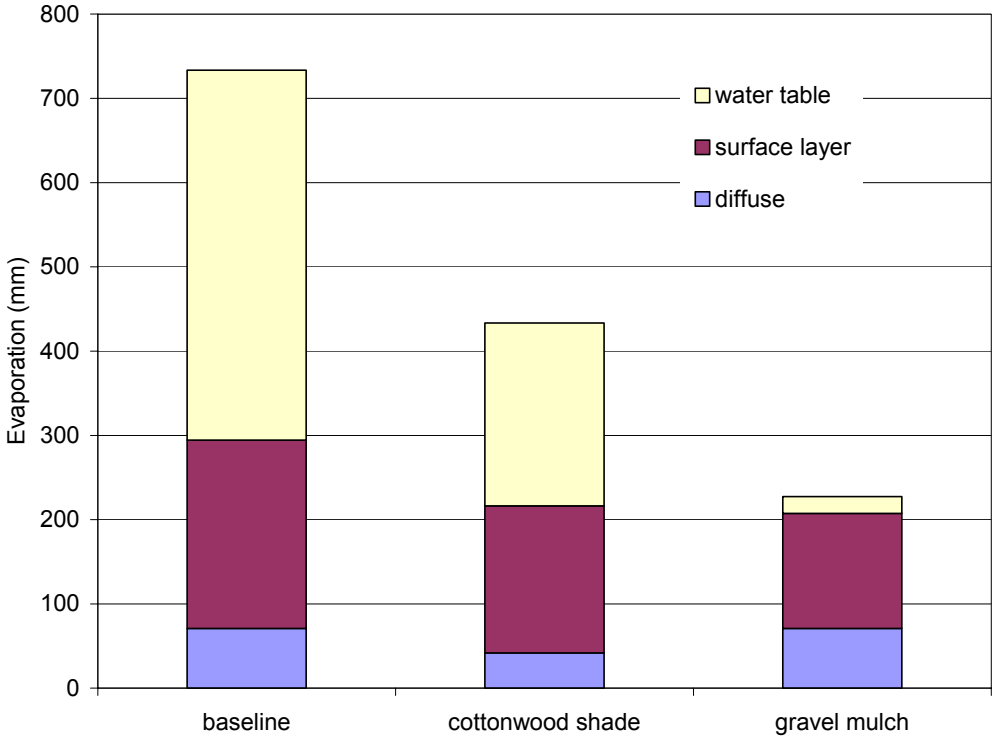

Figure 3.9 – Summary of soil water evaporation for 2006 at Minnow site for baseline, shade and mulch conditions.

Additional results were produced with baseline conditions, but with various values of a constant water table depth. These results are summarized in Figure 3.10. These results show the strong relationship between the distance to the water table and the amount of water table evaporation. For these conditions, water table evaporation is essentially constant when the water table is within about 1 m of the ground surface, and decreases to very low values when the water table is located 2 m or farther from the ground surface. This result will vary with every soil type.

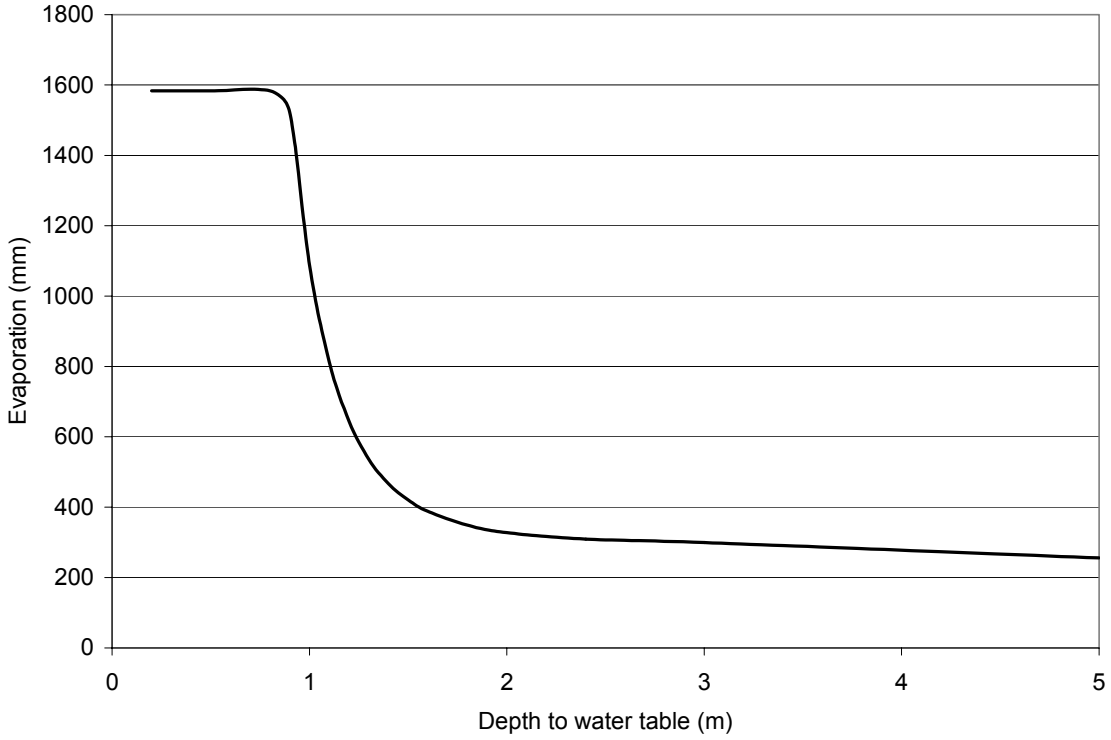

Figure 3.10 - Effect of constant water table depth on evaporation for 2006.

Additional results were produced with three different sets of soil properties to illustrate the impact of the soil type on the predicted evaporation rates. The soils and their properties are described in Table 3.3 and Table 3.4. Soil 1 is the soil used for baseline calculations (Table 3.1). Soil 2 is assigned properties that correspond reasonably well to properties interpreted for the Bosque Del Apache North field evaporation monitoring site (Farfan, 2007). At this site, the top meter of soil consists of layers of silt loam, sand and loam (Stormont et al., 2004). The properties are closest to those denoted by sandy loam D in the numerical water table evaporation simulations (Appendix A). Soil 3 is assigned properties that correspond reasonably well to properties interpreted for the Bosque Del Apache South field evaporation monitoring site (Farfan, 2007). This site has a continuous sand layer overlain by a thin layer of sandy loam (Stormont et al., 2004). The properties are closest to those of the soil denoted as sandy loam E in the numerical water table evaporation simulations (Appendix A).

Table 3.3 – Soil 2 parameters

Parameter	Description	Value
a (mm)	Constant in Gardner's function	-637
N	Constant in Gardner's function	3
χ	Constant in evaporation function	-2.4
FC	Field capacity	0.214
WP	Wilting point	0.072
REW (mm)	Readily evaporated water	8

Table 3.4 – Soil 3 parameters

Parameter	Description	Value
a (mm)	Constant in Gardner's function	-57
N	Constant in Gardner's function	2.3
χ	Constant in evaporation function	-3.7
FC	Field capacity	0.219
WP	Wilting point	0.098
REW (mm)	Readily evaporated water	8

Results for Soil 2 and 3 are summarized in Figure 3.11. The results for Soil 2 reveal a very strong connection to the water table, with the water table evaporation essentially coincident with the reference ET during the entire year. This soil has the ability to transmit water from the water table depth to the surface for the minnow site at a rate that is sufficient to nearly meet the atmospheric demand for water. In contrast, Soil 3 results in virtually no water table evaporation for these conditions.

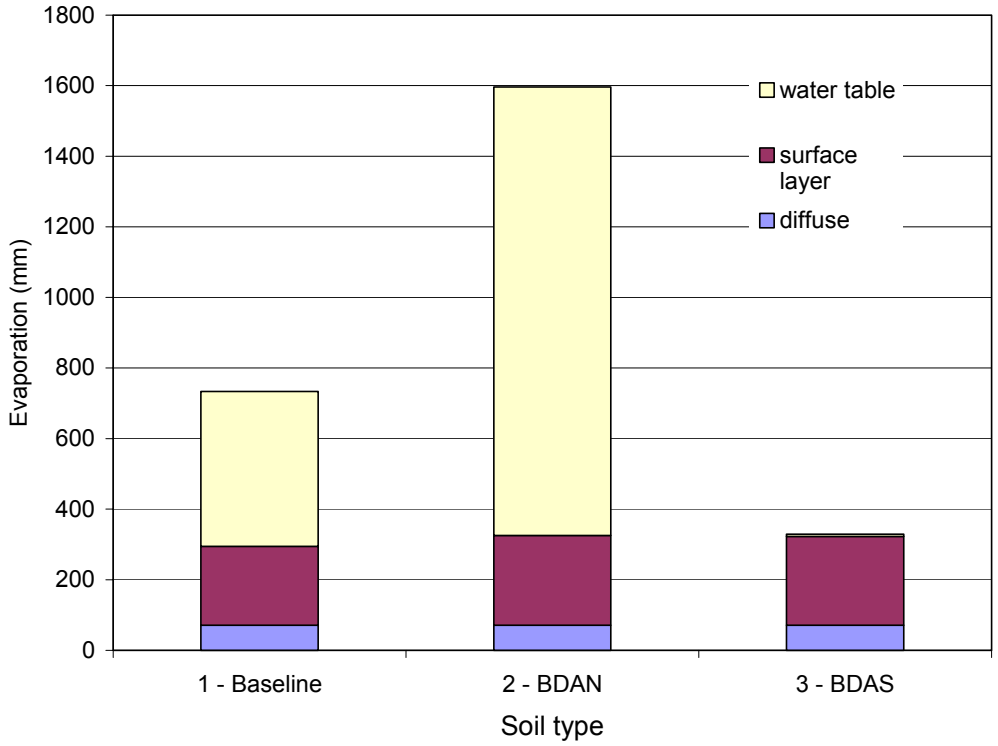

Figure 3.11 – Summary of evaporation estimates for three soils during 2006.

Evaporation estimated for these three soils as a function of constant water table depth is given in Figure 3.12. These results show the striking difference in evaporation as a function of water table depth for the three soils. Soil 2 continues to evaporate from the water table at a maximum rate until the depth to the water table exceeds about 1.2 m, after which point the evaporation rate decreases. Evaporation from Soil 3 decreases immediately as the water table is lowered below the ground surface. The evaporation from Soil 1, the baseline soil, is intermediate between Soil 2 and 3.

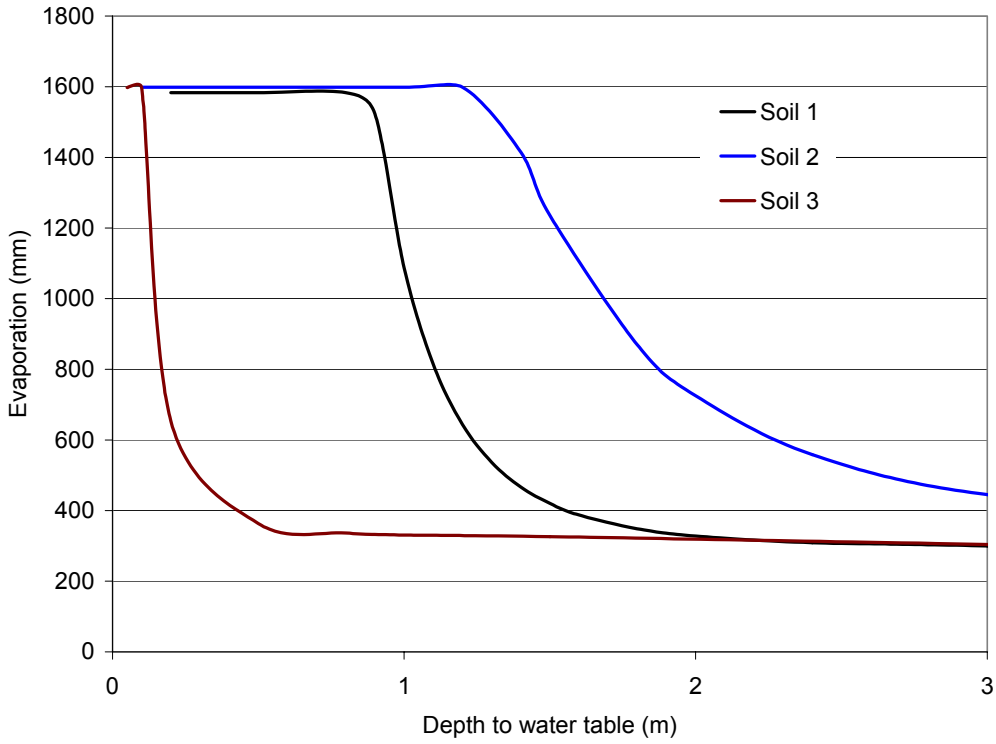

Figure 3.12 - Evaporation as a function of constant water table depth for three soils.

The results above illustrate the importance of soil properties on the connection between the water table and the atmosphere, and the resulting water table evaporation rate. In particular, it is the unsaturated properties of the soil that control water table evaporation. In Figure 3.13, the hydraulic conductivity as a function of suction is given for the three soils. Even though all soils have saturated hydraulic conductivities that are within an order of magnitude (corresponding to suction approaching 0 in Figure 3.13), with increasing suction (that is, unsaturated conditions), the hydraulic conductivities of the soils can be dramatically different. The hydraulic conductivity of Soil 3, for example, dramatically decreases with increasing suction, consistent with the model predictions of little soil water evaporation when the water table falls below the ground surface. Soil 1 and Soil 2 have more similar hydraulic conductivity functions, with a gradual decrease in hydraulic conductivity with increasing suction. The relationship between unsaturated hydraulic conductivity and soil water table evaporation is not necessarily straightforward: even though the model predictions indicate Soil 2 can result in substantially more water table evaporation than Soil 1, Soil 2 has a lower hydraulic conductivity than Soil 1 up until 1000 mm of suction.

The amount of water table evaporation expected for most soils cannot be reasonably estimated based on its textural classification. The properties compiled for different soils in Appendix B reveal that soils that have the same textural classification (e.g., sand, silt loam) can have significantly different hydraulic properties. These differences in properties translate into differences in water table evaporation rates. The conclusion

from all of the simulations of water table evaporation is that there is little correlation between expected evaporation rate and soil type due to the wide range in properties for soils with the same textural classification. An example of this conclusion is given by considering the difference in soil water evaporation predicted for Soils 2 and 3; both soils were classified as sandy loam.

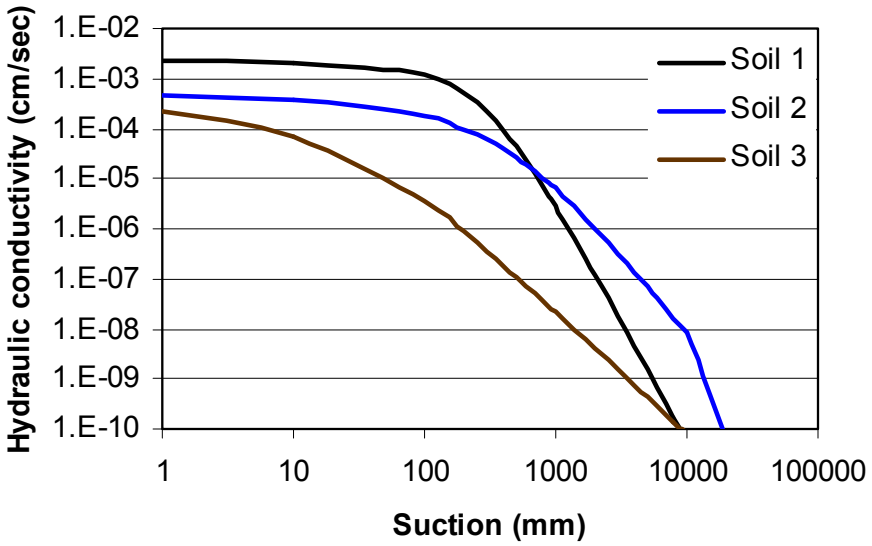

Figure 3.13 – Hydraulic conductivity functions of three soils.

Evaporation estimates are complicated by soil layering. The simulations used to produce the function that describes the relationship between water table evaporation, soil properties and depth were based on homogeneous soil layers. "Effective" hydraulic properties for a single soil layer can be used to represent a layered system; however, the only way at present to estimate these properties is based on inverse numerical simulations (Farfan, 2007).

The best means to obtain soil properties for estimating evaporation is from field measurements. The method developed during the conduct of this project (Stormont et al., 2006; Farfan, 2007) permits effective hydraulic properties of field soils to be estimated from the time history of one or two shallow water content measurements along with corresponding climate data. Effective properties derived from field measurements could be used directly in a model to predict evaporation.

An alternative to the above is to obtain laboratory-derived hydraulic properties from soil samples obtained at the location of interest. Using properties for each identifiable soil layer, numerical simulations could be conducted of the soil profile to estimate evaporation or derive effective hydraulic properties. If there is only one soil type, or if there is one dominant soil type and no low conductivity layers, then it may be possible to directly use the soil properties in an evaporation model.

The least desirable approach for estimating soil properties for use in an evaporation model is to use the textural classification to assign typical hydraulic properties. It has been demonstrated that soils with the same textural classification can have dramatically different evaporation rates.

4. GIS water table evaporation model

The water table evaporation model is made spatially explicit by incorporating the necessary layers in ArcGIS. Water table evaporation is a function of depth to ground water, potential evapotranspiration, and soil properties. As depth to ground water and potential evapotranspiration are also temporally dependent variables, an average monthly model was created. All GIS layers were projected into Universal Transverse Mercator (UTM), Zone 13 with the North American Datum 1983. The projection is good for north to south extents and is used for multiple projects taking place in the Middle Rio Grande (typically, Rio Grande between Cochiti and Elephant Butte). The cell size of the model is 30 meters by 30 meters; although individual data sets may have originated from different cell size resolution. The following sections outline the development of the data used in the model.

4.1 Depth to Water Table

To create a spatially explicit model of water table evaporation, the depth to water table for the Middle Rio Grande corridor must be estimated based on flow in the river and elevation of the ground surface. Additional variables controlling the water table elevation include soil properties, vegetation, riverside drains, domestic and agricultural wells and whether the river is losing or gaining flow. Well data in the bosque, although concentrated in some areas, is insufficient to fully include the additional variables for the entire corridor. River flow is the largest driver for the water table elevation and is the focus for determining depth to water table for the purpose of modeling water table evaporation.

Depth in the river for a given flow rate can be determined based on a hydraulic model such as the Hydrologic Engineering Center River Analysis System (HEC-RAS) developed by the Corps of Engineers. HEC-RAS is a hydraulic model which solves the energy and momentum equations in the direction of flow, along with Manning's uniform flow equation, to determine a water surface profile in an open channel. The United States Bureau of Reclamation (BoR) Sedimentation and River Hydraulics group in Denver creates HEC-RAS models for the Middle Rio Grande utilizing aerial photos every several years. Aerial photos during a low flow period are used to develop cross sections of the channel every 500 feet. The underwater cross section is estimated using Manning's equation and a prismatic channel. Figure 4.2 displays a typical cross section as shown in the HEC-RAS analysis for this study.

HEC-GeoRAS allows for communication between ArcGIS and HEC-RAS. The communication can work both ways such that HEC-RAS cross sections can be developed based on a terrain model in GIS and so that a water surface computed using HEC-RAS can be represented in the GIS. For the purpose of the soil water evaporation model, HEC-GeoRAS is run with an average monthly flow rate.

Flow in the Middle Rio Grande is largely controlled by the releases at Cochiti Dam. Monthly mean flow rate in cfs is obtained from the USGS (http://waterdata.usgs.gov) for gage 8317400 Rio Grande below Cochiti Dam, NM and is shown in Figure 4.2.

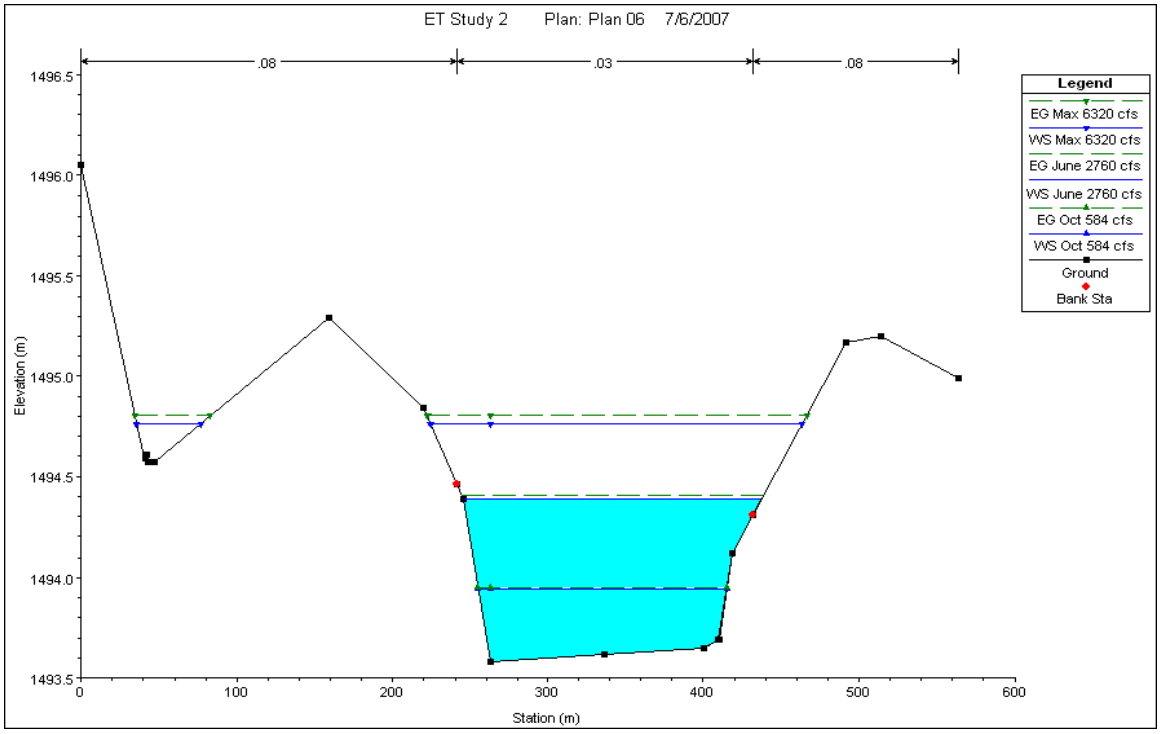

Figure 4.1 Typical cross section in HEC-RAS

USGS 8317400 Rio Grande below Cochiti Dam, NM

Mean of monthly discharge (cfs)

Jan	Feb	Mar	Apr	May	Jun	Jul	Aug	Sep	Oct	Nov	Dec
803	925	1,160	1,850	2,970	2,760	1,560	891	708	584	839	865

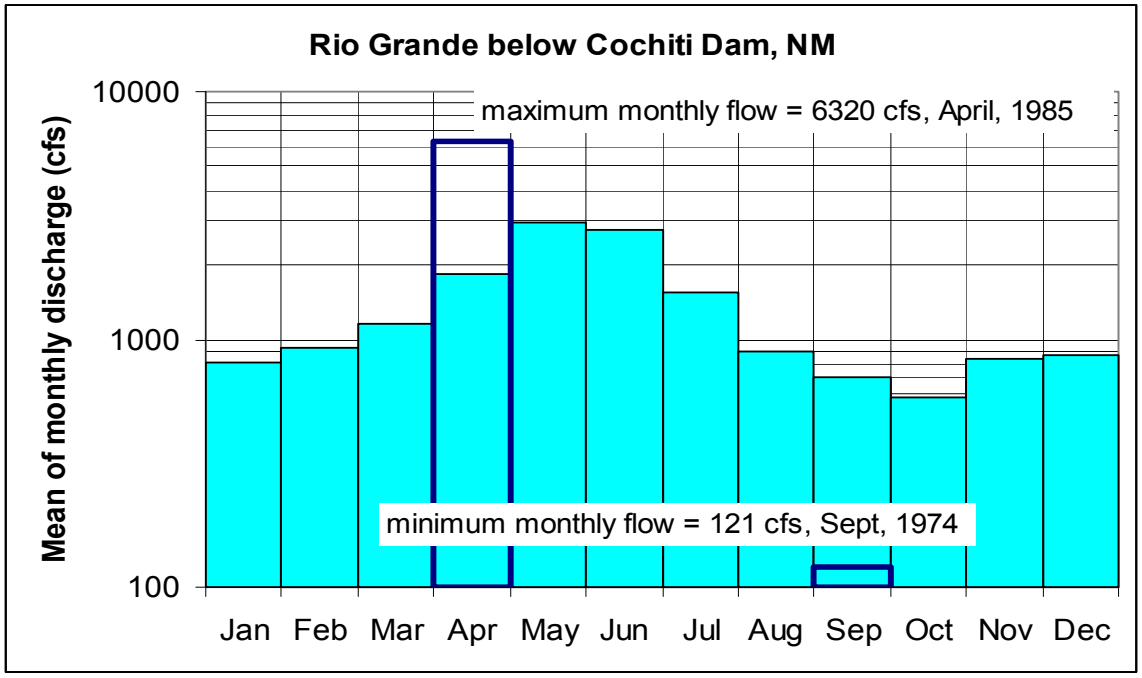

Figure 4.2 Mean monthly discharge at Rio Grande below Cochiti Dam, NM

The maximum monthly flow recorded below Cochiti Dam was 6320 cfs during April, 1985 while the lowest monthly flow occurred in September, 1974 at a rate of 121 cfs. HEC GeoRas was run for each average monthly flow rate as well as the maximum and monthly flow rates to create a total of 14 possible water surfaces for the Middle Rio Grande. Figure 4.1 shows the results for several of the flow rates for this study. It should be noted that HEC-RAS assumes an entire cross section to fill with water from bottom to top regardless of whether the flow can actually reach the entire cross section. HEC-RAS allows a user to code in levees and ineffective areas to remedy such issues. Levee and ineffective flow areas were not included in the RAS model for this study.

GeoRAS creates a triangular irregular network (TIN) representing the water surface. The TIN is converted to a raster to enable analyses with other data rasters. To create a ground water surface, a horizontal piezometric surface is assumed. This surface is created by using a series of focal mean functions within ArcGIS such that the horizontal piezometric surface is perpendicular to the river flow. The depth to the water table is then calculated for each 30 m by 30 m grid cell as the difference between the terrain model and the water surface. The terrain model was created using the BoR cross sections as they extend throughout the riparian forest. This process is repeated for each flow rate – in this case, twelve average monthly flow rates and the maximum and minimum monthly flow rates. Figure 4.3 zooms in on a section of river to illustrate the relationship of the terrain model and the water surface.

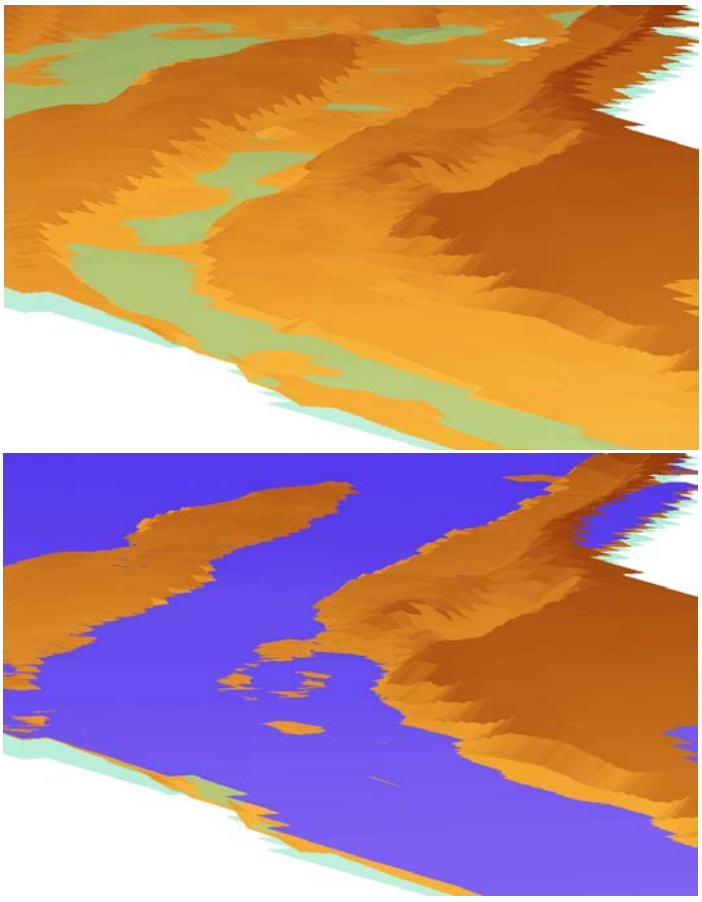

Figure 4.3 3-D rendering of river terrain model with low and high flow rates

Additional development of the terrain model was out of the scope of this study. The 30 meter digital elevation model (DEM, available from the USGS seamless data distribution website: seamless.usgs.gov) is projected into the UTM coordinates used for this work. As the river channel is approximately 600 feet, or 180 m, wide, it was assumed that the 30 m DEM would be adequate to define the river channel. The 30 m DEM defines the valley well as shown in Figure 4.4. However, due to averaging and the many islands and sandbars in the channel, the channel is often

shown as about 1 foot lower in depth than the surrounding area. Thus, the channel is not adequately defined by the 30-m DEM. The problem is not alleviated by using the USGS 10-m DEM as the 10-m DEMs are not developed by higher resolution data and are simply developed by using an interpolation routine. The development of an accurate terrain model for this long thin river corridor presents many challenges and should be the subject of future research.

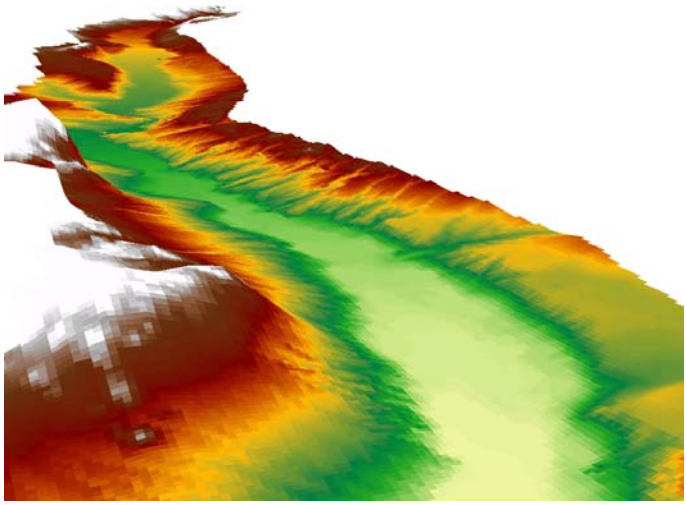

Figure 4.4 USGS 30-m DEM

4.2 Potential Evapotranspiration

For the spatially distributed water table evaporation model, average monthly (spatially distributed) values of potential evapotranspiration (PET) were needed. There are a number of different methods to calculate potential evapotranspiration (PET). The water table evaporation estimation method developed as part of this work utilizes Penman's equation to calculate PET. Penman's equation is a function of net radiant energy. Net radiant energy is not readily available as a function of space averaged over time (although, net radiant energy as a function of space can be determined from satellite imagery). In fact, the creation of PET values as a function of space and time are the subject of many studies. For the purposes of this work, pan evaporation data were used to develop a rasterized layer of average PET for each month.

Average monthly pan evaporation values can be acquired from the Western Regional Climate Center located at the Desert Research Institute in Nevada (http://www.wrcc.dri.edu/htmlfiles/westevap.final.html#NEW%20MEXICO) or the New Mexico Climate Center (http://weather.nmsu.edu). The coordinates for each pan evaporation station are available through linked pages. A table of monthly pan evaporation data along with latitude and longitude coordinates of the sites was created in dBase format so that the table could be used in ArcGIS. The table required review as some stations had nonsensical data and many stations had a value of zero for the winter months as many stations do not measure pan evaporation during winter months. A "0.00" total indicates no measurement is taken. The data were removed for individual months and stations as appropriate.

Pan evaporation surfaces were created using the point data and the inverse distance weighted routine in ArcGIS. The inverse distance weighted routine interpolates the value

of pan evaporation in a grid cell by weighting those pan evaporation stations closer to the grid cell more heavily than those pan evaporation stations farther from the grid cell. In this manner the average pan evaporation for each month was determined. The rasterized layers of monthly pan evaporation were projected into UTM, resampled as 30 m grid cells, and cut to the Middle Rio Grande corridor. Figure 4.5 shows a typical pan evaporation surface. The July pan evaporation surface varies from 8.5 to 14.3 inches (216 to 363 mm) with the highest values occurring at Elephant Butte dam.

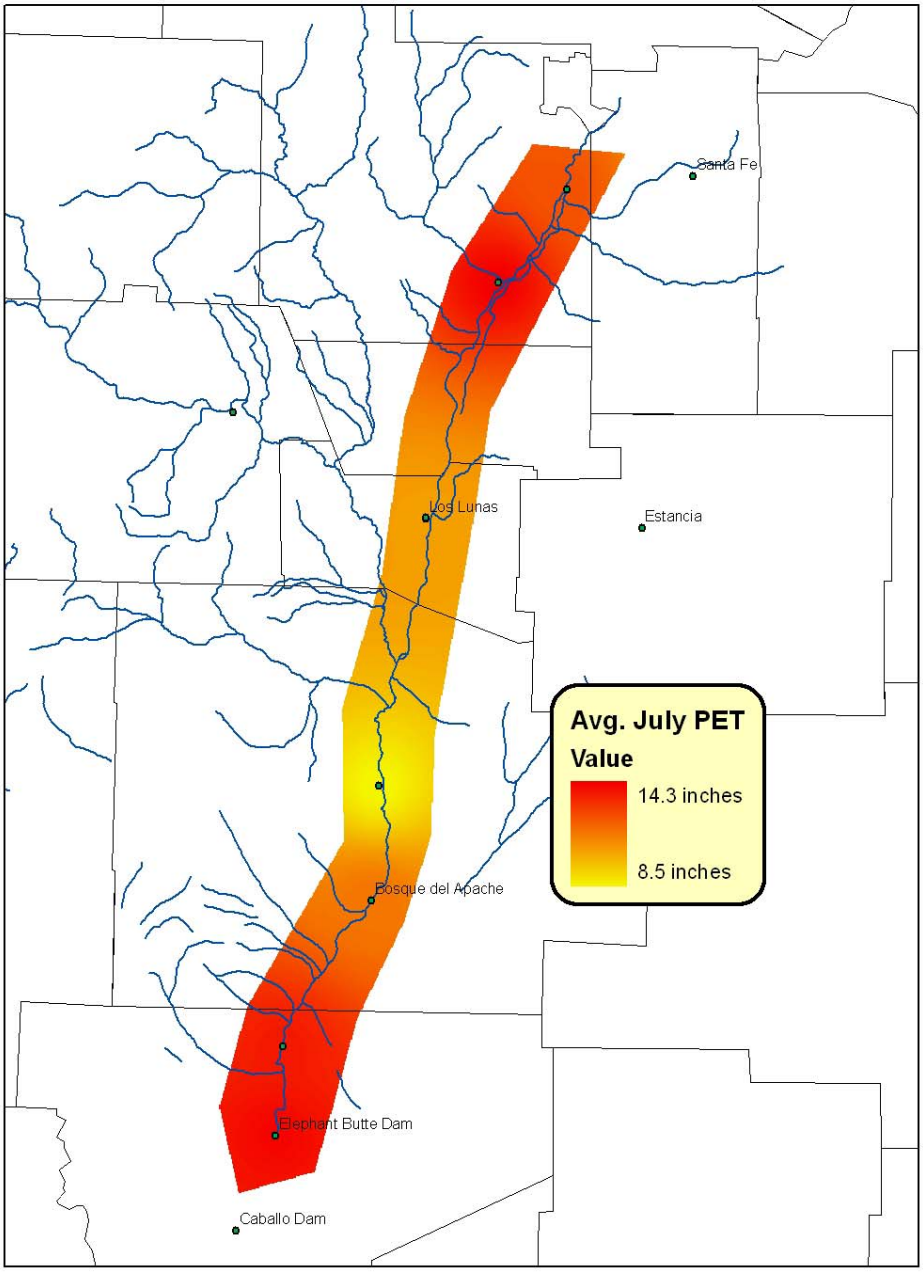

Figure 4.5 Average monthly pan evaporation in Middle Rio Grande for July

As stated on the Western Regional Climate Center website:

> "Standard daily pan evaporation is measured using the four-foot diameter Class A evaporation pan. The pan water level reading is adjusted when precipitation is measure to obtain the actual evaporation. Most Class A pans are installed above ground, allowing effects such as radiation on the side walls and heat exchanges with the pan material. These effects tend to increase the evaporation totals. The amounts can then be adjusted by multiplying the totals by 0.70 or 0.80 to more closely estimate the evaporation from naturally existing surfaces such as a shallow lake, wet soil or other moist natural surfaces."

The water table evaporation model requires the use of PET determined by Penman's equation. Pan evaporation has been compared to Penman's PET by a number of researchers. Typically, PET is equal to 70-85 percent of the pan evaporation (Linacre, 1993; Brouwer and Heibloem, 1986). However, a previous study (http://weather.nmsu.edu/hydrology/ratiopaneto.htm) of New Mexico data is available on the New Mexico Climate Center web page. Figure 4.6 shows the ratio of PET to pan evaporation to oscillate around 1.0.

http://weather.nmsu.edu/hydrology/ratiopaneto.htm

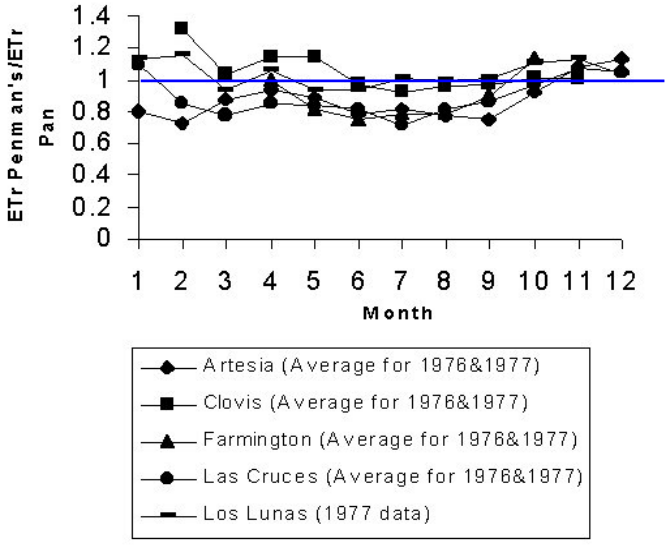

Data from Sammis, T. W., E. G. Hanson, C. E. Barnes, H. D. Fuehring, E J. Gregory, R. F. Hooks, T. A. Howell, and M. D. Finkner. 1979. Consumptive use and Yields of crops in New Mexico. New Mexico Water Resources Research Institute. report 115 pp1-108

Figure 4.6 Comparison of pan evaporation and Penman's PET in New Mexico

Thus for the purposes of this model the pan evaporation data is assumed to closely approximate the PET as calculated by the Penman equation. By utilizing the pan evaporation data, PET can vary with time and space. Furthermore, if a future study generated the data to more accurately compare pan evaporation with PET, coefficient grids could be created and applied at that time.

4.3 Soil Properties

Soil properties in the bosque vary greatly with space. Spatially varied datasets containing soil properties, such as the State Soil Geographic (STATSGO) data set, lump the riparian soils into a single group. Well cores throughout the bosque have been analyzed by many but are not readily available. Furthermore, the well cores indicate the layered nature of the riparian soils and the unpredictability of small clay lenses that would alter water table evaporation significantly. Detailed soils analyses of the instrumented sites were done as part of this study. Utilizing the results of those soils analyses and the parameters used in the empirical water table evaporation model, typical bosque soil parameters were developed. The soil property grids can be filled with single values such that the soil is not a function of space or the grids can be filled with site specific, spatially varying data. To demonstrate the utility of the model, soil properties were assumed to be spatially constant as shown in Figure 4.7.

4.4 GIS Model

The GIS model (Figure 4.7) applies the function relating water table evaporation to depth to ground water, PET, and soil properties for a monthly time step.

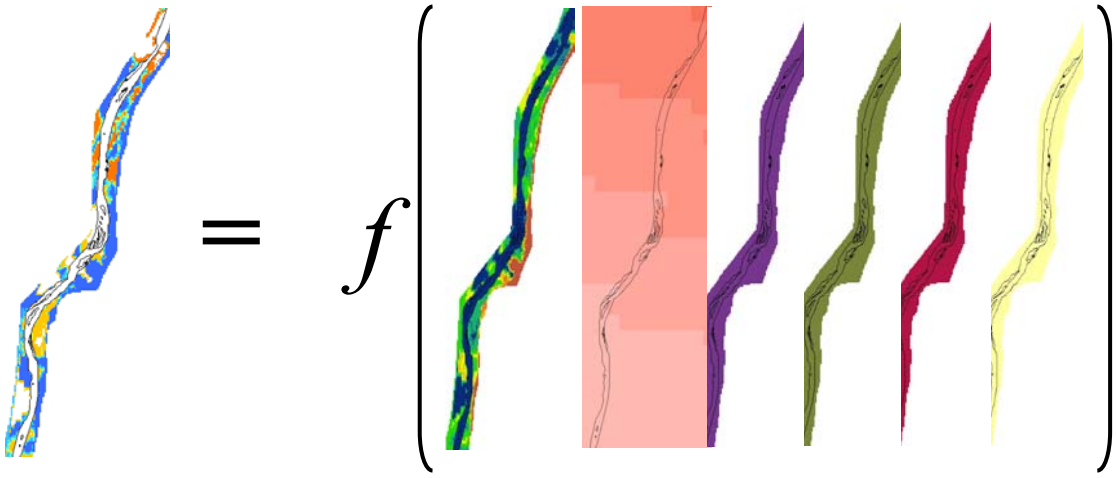

Evap = f (Depth to ground water, PET, soil properties)

Figure 4.7 Spatially distributed model for calculating water table evaporation

The function, $E = \text{Min}\,(PETR\, e^{\chi}\, Ksat\, [(-a\,\pi)/(L\,N \sin(\pi))]^{N}, 0.85\,PET)$ is detailed in Chapter 2. PETR is the PET Ratio and is equal to Penman's PET divided by 1. L is depth to ground water and a, N,chi, and Ksat are variables related to soil properties. As evidenced in Figure 4.7, the evaporation grid, depth to ground water grid, and PET grid show spatial variability. The depth to ground water and PET grids were determined as outline earlier in this chapter; however, an adjustment had to be made to the depth to ground water grid.

The ground elevation raster minus the water surface elevation results in negative values in the river channel and, possibly, in low lying bosque area. These two areas should be treated differently, as the objective of this work is to calculate potential water table evaporation in the bosque. Thus, the river is excluded from the analysis using a 'setnull' function. Negative depth to ground water values in the bosque result in open water evaporation and for the purposes of this model are treated the same as very shallow ground water.

The empirical model presented in Chapter 2 utilizes Gardner's function which produces non-meaningful results for ground water depths of zero to about 0.10 m. Thus, all values less than 0.10 m are set to 0.10 m for the purpose of calculating the Gardner function. For this shallow ground water, the calculated evaporation is simply a function of PET and the depth to ground water is not a variable. The soil parameters determine when the depth to ground water is utilized in the function, generally greater than about 0.5 m.

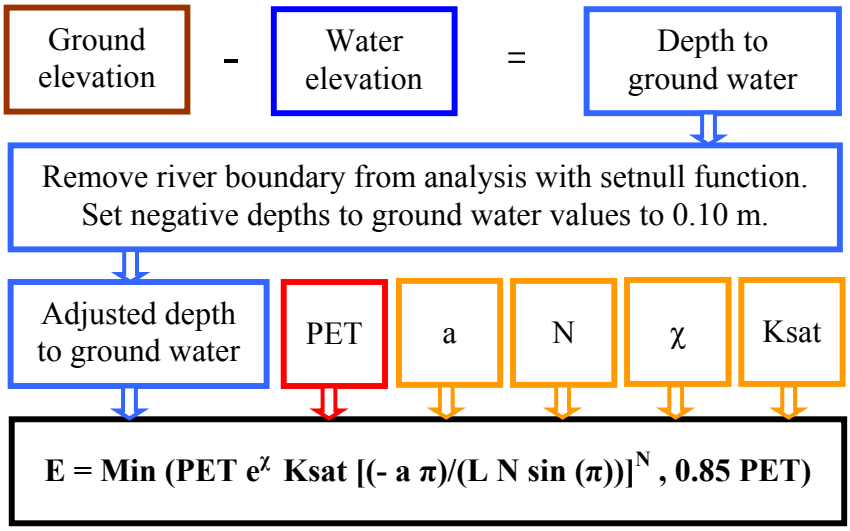

Figure 4.8 Conceptual spatially varied model to calculate water table evaporation

These series of functions can be applied for each month using the Raster Calculator in ArcGIS. To automate the process and eliminate the redundancy of repeating steps for each month, the ModelBuilder in ArcGIS was used to automate the spatially dependent calculations.

This model provides a tool for researchers and managers to estimate water table evaporation in the bosque in the absence of vegetation. By doing so, areas of higher water table evaporation can be identified as areas where water savings are less likely due to bosque management that includes vegetation removal and vice versa. The actual values of water table evaporation depend of the accuracy of the data for each cell. As the soil properties have not been analyzed for each cell, it is not reasonable to consider the predicted values of the water table evaporation as representing actual evaporation.

However, the relative values of water table evaporation are more important than the actual values from the perspective of bosque management.

The model can be improved by:

- an improved terrain model,
- an improved HEC-RAS model,
- additional field data to more accurately populate the soil property grids,
- additional research on potential evapotranspiration, and
- additional field data to more accurately represent the piezometric surface as a function of flow rate.

4.5 Model Application

The depth to ground water was determined by calculating a water surface profile for each average monthly flow rate from Cochiti Dam and assuming a horizontal piezometric surface. The monthly potential evaporation grids were created using pan evaporation data. The soil property grids were populated with values from representative bosque soils. Further research resulting in improved data for any of the variables can easily be incorporated into the model at a later date.

The model was used to determine the average monthly water table evaporation in the absence of vegetation. The soil parameters are listed in Chapter 3. Table 4.1 lists spatial averages for each month using Soil 1 (Baseline soil parameters, Table 3.1). Low values are not reported as they are zero every month. The spatial average, high, and standard deviation are shown in Figure 4.9.

Table 4.1 Modeled water table evaporation rates for Soil 1 with the absence of vegetation

month	Modeled water table evaporation (mm/day)		
	average	high	Standard deviation
Jan	1.4	2.5	0.9
Feb	2.1	3.8	1.3
Mar	3.0	5.4	2.0
Apr	4.1	7.7	2.9
May	4.3	8.6	3.3
Jun	5.0	10.0	3.8
Jul	4.9	9.9	3.4
Aug	4.6	7.9	2.9
Sep	3.8	7.0	2.4
Oct	2.6	4.7	1.7
Nov	1.8	2.9	1.1
Dec	1.2	1.9	0.8

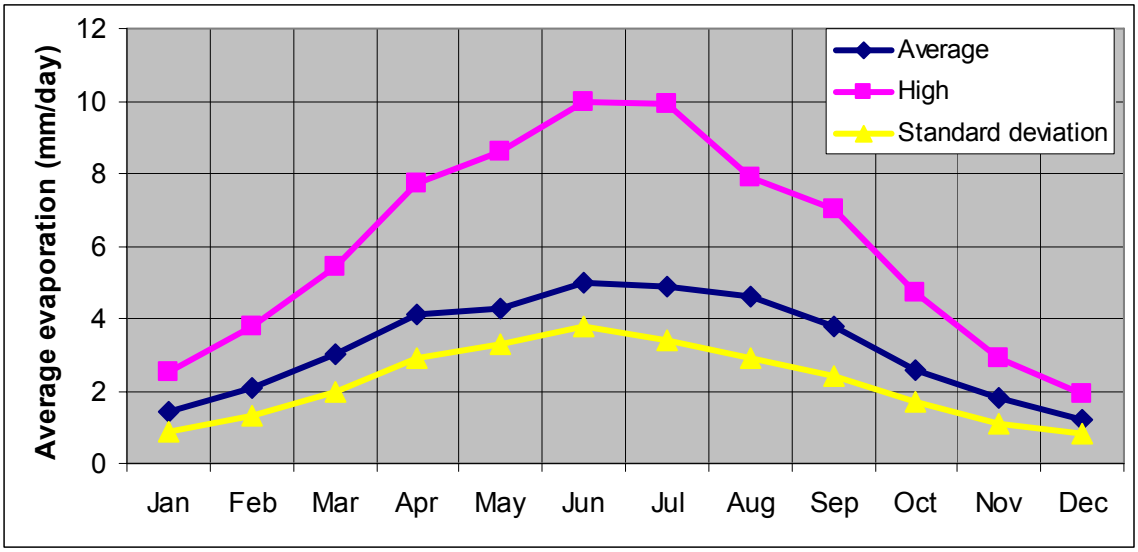

Figure 4.9 Estimated evaporation rates using spatially distributed model for Soil 1

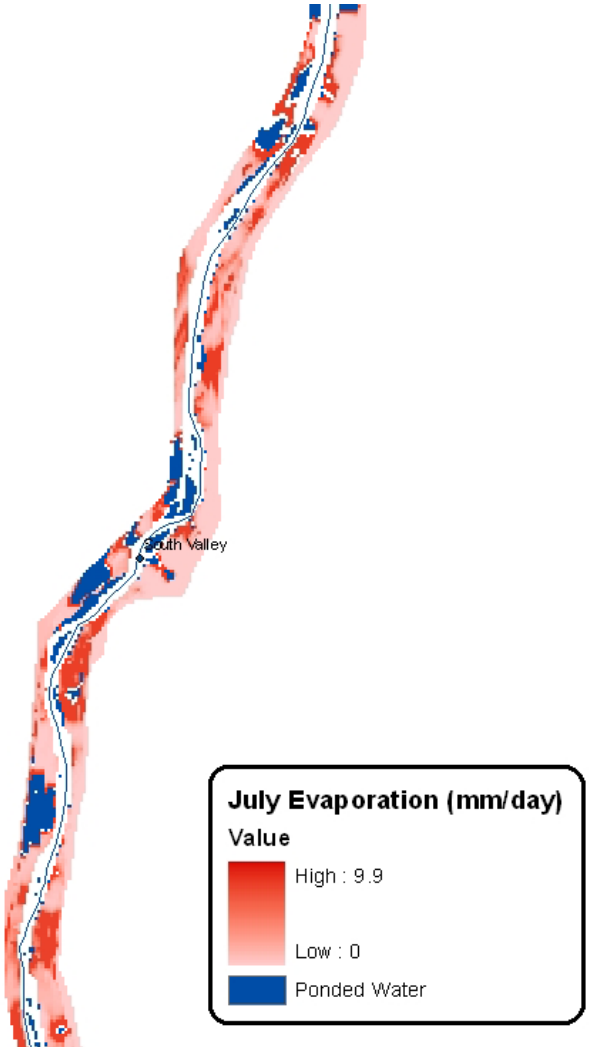

Figure 4.10 Model results for Soil 1

The results are generally as expected, with very low evaporation rates in the winter months and high evaporation rates in the summer months. The average April flow rate exceeds that in July and August resulting in shallower ground water depths, however the higher evaporative demand in the atmosphere has a greater effect resulting in higher water table evaporation during July and August in comparison to April. The standard deviation is similar to the average for each month indicating a very high degree of variability and a skew to shallow ground water depths. The HEC-RAS analysis for this study contributes to the overestimation of areas with shallow groundwater depths by not correcting the RAS model with levees and ineffective flow areas.

Figure 4.10 shows the model results for July for Soil 1. The darker red areas indicate the highest area of water table evaporation. Bosque management in such areas should consist of shade and mulch to minimize water losses. The blue areas represent areas resulting in

ponded water with model execution. For modeling purposes, such areas were assigned 0.1 m water table depth, resulting in high evaporative rates. Improvement to the terrain model might eliminate many of the ponded water areas. Further review of Figure 10 does not lend insight into generalizations regarding areas resulting in high or low water table evaporation. All of the model results for the entire analyzed riparian corridor (as well as input) are available in Appendix D such that smaller areas of concern can be reviewed. Figure 4.11 illustrates the modeled evaporation for the Middle Rio Grande. It should once again be emphasized that the model provides comparative results and not necessarily absolute values.

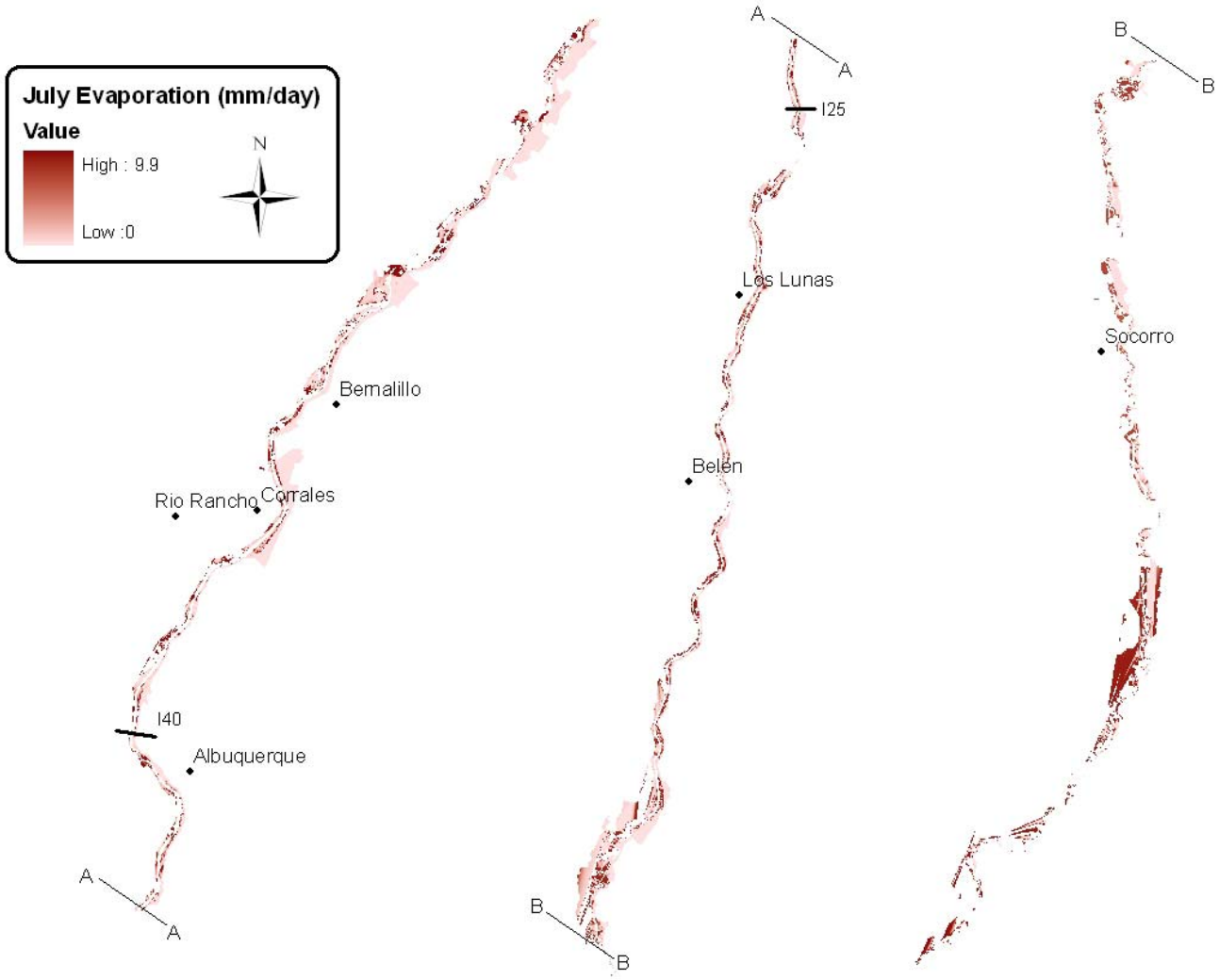

Figure 4.11 Modeled water table evaporation in the absence of vegetation, Soil 1.

To further investigate the sensitivity to river flow rate, the low flow was combined with a high PET grid and with a low PET grid. The high flow was combined with April PET and July PET as high monthly flows are a result of snow melt and it would not make

sense to combine the high flow with a low PET grid. The model can be used to make any number of combinations of flow rate, PET, and soil parameters. The results for these suggested combinations are presented in Table 4.2.

Table 4.2 Modeled water table evaporation rates for Soil 1 with the absence of vegetation

Flow, PET	Modeled water table evaporation (mm/day)		
	average	high	Standard deviation
Min, Jun	2.7	10.0	3.1
Min, Jan	0.6	2.5	0.7
Max, Apr	4.7	7.7	2.6
Max, July	5.7	10.0	3.1

For the minimum flow rate, the average water table evaporation rates decreased significantly in comparison with the same months in Table 4.1, indicating the influence of the water table depth. Likewise, for the maximum flow rate, the average water table evaporation rates increased. The high water table evaporation rates are essentially the same as the rates are controlled in large part by the PET. The 5.7 mm/day computed by spatially averaging the cells for a maximum flow rate with a high PET should be considered near an upper bound for possible water table evaporation (spatially averaged) in the absence of vegetation for the duration of a month. Larger flows, resulting in shallower ground water can cause higher daily evaporation rates, but not for the course of a month.

Table 4.3 displays similar statistics for different soils types. The soil parameters for Soils 1, 2, and 3 are presented in Chapter 3. Soil 1 is a reasonable representative bosque soil. Soil 2 has hydraulic properties that are expected to be conducive to evaporation and should evaporate more than Soil 1. Soil 3 is a sandy, well drained soil and should not evaporate as much as the others. The model captures these differences in the soil types. Combining Soil 2 with the maximum flow rate and a high PET can result in an even higher evaporation rate than the 5.7 mm/day that was suggested as an upper bound for the duration of a month. Soil 3 produces substantially less evaporation than the other soils. These results illustrate the importance of the soil type and hydraulic characteristics on the amount of water depleted by soil water table evaporation.

Table 4.3 Modeled water table evaporation rates for various soils, absence of vegetation

Month	Soil	Modeled water table evaporation (mm/day)		
		Average	High	Standard deviation
June	1	5.0	10.0	3.8
	2	6.3	10.0	3.0
	3	0.7	10.0	1.5

October	1	2.6	4.7	1.7
	2	3.1	4.7	1.4
	3	0.2	4.7	0.5

4.6 Conclusion

The model successfully applies the equations of Chapter 2 and the soil properties of Chapter 3 to estimate spatially distributed values of water table evaporation in the absence of vegetation. The model responds appropriately to changes in water table depths, PET, and soil parameters. The model can be used as a management tool to determine areas of highest and lowest water table evaporation rates for a given flow rate, PET, and soil characteristics. The model's intent is to provide values for the purpose of comparisons, not to calculate exact values of water table evaporation. Appendix D is a DVD containing the ArcGIS Model and the interchange files for all grids used in this study.

5 References

Allen, R.G., Pereira, L.S., Raes, D. and Smith, M., 1998. "Crop evapotranspiration: Guidelines for computing crop requirements." *Irrigation and Drainage Paper No. 56*, FAO, Rome, Italy.

Allen, R.G., Pruitt, W.O., Raes, D., Smith, M. and Pereira, L.S., 2005. "Estimating Evaporation from Bare Soil and the Crop Coefficient for the Initial Period Using Common Soils Information," ASCE, *Journal of Irrigation and Drainage Engineering*, Vol. 131, No. 1, p. 14 – 23.

Brouwer, C. and M. Heibloem, 1986. " Irrigation Water Management: Irrigation Water Needs," a manual prepared jointly by International Institute for Land Reclamation and Improvement and FAO Land and Water Development Division, Part 2, Chapter 3.

ESA, 2003. ESA Collaborative Program Ad Hoc Committee on Net Depletions, *State of the Science Report*, December.

Farfan, E., 2007. "Estimating Soil Water Evaporation Using Nonlinear Inverse Theory", Dissertation, University of New Mexico.

Fayer, M., 2000. *UNSAT-H Version 3.0: Unsaturated Soil Water and Heat Flow Model – Theory, User Manual, and Examples*, Report No. PNNL-13249, Pacific Northwest Naitonal Laboratory, Richland, WA.

Gardner, W.R. (1958). "Some steady-state solutions of the unsaturated moisture flow equation with application to evaporation from a water table". *Soil Science*, vol. 85, no. 4, pp. 228-232.

Hillel, D. (1982). Soil Physics. Academic Press, London.

Jury, W.A., Gardner, W.R., and Gardner, W.H., 1991, Soil Physics, John Wiley & Sons, New York.

Linacre, E.T. 1993. "Data-sparse estimation of lake evaporation using a simplified Penman equation". *Agricultural & Forestry Meteorology*, Vol. 64, pp. 237-56.

Campbell, G.S. and J. Norman (1998). Environmental Biophysics, Springer.

McDonnell, D., 2006. Scaling Evapotranspiration in the Middle Rio Grande, Dissertation, University of New Mexico.

Mutziger, A.J., Burt, C.M., Howes, D.J., and Allen, R.G., 2005. "Comparison of Measured and FAO-56 Modeled Evaporation from Bare Soil", ASCE*, Journal of Irrigation and Drainage Engineering*, Vol. 131, No. 1, p. 59-72.

Sammis, T. W., E. G. Hanson, C. E. Barnes, H. D. Fuehring, E J. Gregory, R. F. Hooks, T. A. Howell, and M. D. Finkner. 1979. "Consumptive use and Yields of crops in New Mexico". New Mexico Water Resources Research Institute. report 115 pp1-108

Stormont, J.C. and Anderson, C.E., 1999. Capillary Barrier Effect of Fine-over-coarse Soils, *Journal of Geotechnical and Geoenvironmental Engineering,* ASCE, Vol. 125, No. 8, pp. 641 - 648.

Stormont, J., Coonrod, J., Farfan, E., and Harp, D., 2004. "Bosque Soil Evaporation Monitoring and Modeling Report for Year 1," Department of Civil Engineering, report to the ESA Collaborative Program, October 18.

Stormont, J., Coonrod, J., Farfan, E., Harp, D., 2006. "Bosque Soil Evaporation Monitoring and Modeling Report for Year 2," Department of Civil Engineering, report to the ESA Collaborative Program, February 2.

Stormont, J., Coonrod, J., 2005. "Bosque Soil Evaporation Monitoring and Modeling Status Report on Field Monitoring," Department of Civil Engineering, report to the ESA Collaborative Program, May 18

UNM, 2007. "Urban Flood Demonstration Project Annual Report," University of New Mexico, Department of Civil Engineering, report to US Corps of Engineers.

Wythers, K.R., W.K. Lauenroth, and J.M. Paruelo, 1999. "Bare-Soil Evaporation Under Semiarid Field Conditions", *Soil Science Society of America Journal*, Vol 63, pp. 1341-1349.

Zammouri, M., 2001. "Case study of water table evaporation at Ichkeul Marshes", ASCE, *Journal of Irrigation and Drainage Engineering,* ASCE, Vol. 127, pp. 265-271.

Additional material provided with Final Report

Appendix A – Numerical analysis of soil water table evaporation (AppendixA.pdf). This appendix includes a number of sub-appendices that contain soil hydraulic properties and calculated soil water table evaporation rates.

Appendix B - Calibration of FAO-56 method for location in the Middle Rio Grande Valley (AppendixB.pdf). This appendix includes field data used to calibrate the FAO-56 model.

Appendix C – Excel spreadsheet of total soil water evaporation model based on FAO-56 including water table evaporation (TSWE 7-5-07.xls)

Appendix D – GIS model of water table evaporation (multiple files on separate DVD)